Validation of Simplified Level 2 Prototype Processor Sentinel 2 Fraction of Canopy Cover, Fraction of Absorbed Photosynthetically Active Radiation and Leaf Area Index Products over North American Forests

Richard Fernandes, Francis Canisius, Gang Hong, Camryn MacDougall, Hemit Shah, Lixin Sun, Lynsay Spafford, Patrick Osei Darko, Fred Baret, Luke Brown, Jadu Dash, Courtney Meier, Marie Weiss

Abstract

Canopy biophysical variables such as the fraction of canopy cover (fCOVER), fraction of absorbed photosynthetically active radiation (fAPAR), and leaf area index (LAI) are widely used for ecosystem modelling and monitoring. The Sentinel 2 mission was designed for systematic global mapping of these variables at medium (≤30m) resolution using imagery from the Multispectral Instrument. The Simplified Level 2 Prototype Processor (SL2P) is available as a baseline mapping solution. Validation over limited sites indicates SL2P generally satisfies user requirements for all three variables over crops but underestimates LAI over forests. In this study, Sentinel 2 fAPAR, fCOVER and LAI products from SL2P were validated over 281 sites representative of most North American forest ecozones and compared with coarse resolution products of known performance. In addition to meeting the Committee of Earth Observing System Level 3 validation requirements for these areas, our study also explores the relationship between bias in SL2P products and canopy clumping.

SL2P was implemented within the LEAF-Toolbox in Google Earth Engine both for efficiency and due to bugs in the Sentinel Application Platform implementation. SL2P underestimates LAI by 20% to 50% over forests with LAI>2; in agreement with other studies and with comparisons to MODIS products. SL2P bias for fCOVER and fAPAR transitions from ~0.1 at low values to ~-0.1 at high values. Precision error was ~0.5 for LAI and slightly less than ~0.1 for fCOVER and fAPAR at one standard deviation. Thematic uncertainty was dominated by bias for LAI with LAI>2 and slightly greater than precision for other variables Target user requirements were satisfied for 48% of LAI, 37% of fCOVER and 31% of fAPAR comparisons. Quantitative evidence supporting the effect of clumping on bias was weak but scatter plots indicated larger negative LAI biases over northern latitude sites where canopies exhibited greater clumping. These results suggest SL2P LAI biases may be reduced by using a heterogeneous radiative transfer model for calibration. In the meantime, users of SL2P for forest mapping should apply a bias correction for LAI or rely on effective LAI, fAPAR or fCOVER

1. Introduction

A primary goal of the Sentinel-2 mission (S2) is the systematic mapping of canopy variables, including the fraction of canopy cover (fCOVER) , fractional of absorbed photosynthetically active radiation (fAPAR), and leaf area index (LAI), using measurements from a Multispectral Instrument (MSI) on a constellation of polar orbiting satellites (ESA Sentinel-2 TEAM, 2007). The European Space Agency (ESA) sponsored the development of the Simplified Level 2 Prototype Processor (SL2P) for mapping these variables using Level 2a surface bi-directional reflectance (BRF) products derived from MSI data (Weiss and Baret, 2016). SL2P versions are implemented in the SNAP - ESA Sentinel Application Platform v2.0.2 (http://step.esa.int), used with the European Union SEN4CAP agricultural sustainability project (http://esa-sen4cap.org/), and the open source LEAF-Toolbox (Fernandes et al., 2021) implemented in Google Earth Engine (GEE), used by the Government of Canada Cumulative Effects Monitoring Programme (Janzen et al., 2020).

S2 mission requirements correspond to the most stringent requirements currently under review by the Global Climate Observing System (GCOS, 2019; "Goal" in Table 1). The Copernicus Global Land Service (CGLS) has also identified requirements considered acceptable by many downstream services (Sanchez-Sapero and Martinez-Sanchez, 2022; "Target" in Table 1). SL2P products have been validated over a limited number of sites (<30); corresponding to Committee of Earth Observing System Level 2 (CEOS, https://lpvs.gsfc.nasa.gov/) (Table 2). SL2P generally satisfies target requirements for crops (Djamai et al. 2018; Hu et al. 2020; Brown et al., 2020) but systematically underestimates LAI and fAPAR over dense forests (Putzenlechner et al., 2019; Brown et al., 2021). Brown et al. (2021) hypothesised the LAI underestimation was due to spatial clumping of foliage not accounted for within SL2P. This also raises the concern that clumping may also result in greater uncertainty of SL2P fAPAR and fCOVER estimates. Forests, especially those at high latitudes, exhibit substantial clumping (He et al. 2012) so simultaneous validation of SL2P LAI, fCOVER and fAPAR over a broad geographical range of forests is critical to understand the limitations of SL2P and to prioritise improvements.

Here SL2P is validated using in-situ reference measurements (RM) for all forest ecological zones of North America (Commission for Environmental Cooperation, 2022), except wet tropical forests, and compared to coarse resolution Moderate Resolution Imaging Spectrometer (MODIS) and CGLS products that have been previously validated. Our goal is to: I) quantify the accuracy (A), precision (P) and uncertainty (U) of SL2P LAI, fAPAR and fCOVER estimates over typical North American Forests ii) determine if indeed the uncertainty of each variable is related to the amount of canopy clumping and iii) provide good practices for achieving a CEOS Level 3 validation of medium resolution vegetation biophysical variable products.

Table 1. Product definitions (GCOS, 2019) and user requirements for thematic performance.

Variable	Definition	Goal	Target
fAPAR	Fraction of absorbed photosynthetically active radiation by green vegetation for a given solar illumination condition.	5%	max(10%,0.05)
fCOVER	Fraction of ground covered by green vegetation.	5%	max(10%,0.05)
LAI	Half the total foliage area per unit horizontal ground area.	10%	max(15%,0.5)

This study considers North American forests due to the aforementioned underestimation observed by SL2P in forests over a limited (<30) number of sites. A larger in-situ sample and product intercomparison is recommended by CEOS (i.e. Level 3) to quantify the structure of errors for forests as a function of the RM value. SL2P has yet to achieve CEOS Level 3 due limited in-situ sites and the computational demands of sufficient generating products for intercomparison. A new Canadian field campaign was conducted to address the issue of limited in-situ sampling. To facilitate product intercomparison, SL2P was also implemented in GEE to produce products over a replicate sample of 100km x 100km regions of all 18 forest ecozones. Even so, this study does not evaluate the temporal stability of SL2P products as, prior to 2019, imagery over North America has not systematically processed by ESA.

Datasets for stratification and in-situ validation are described in Section 2. Methods for performing validation and intercomparison are described in Section 3 with emphasis on quantifying A, P and U as a function of product value and also the uncertainty in these statistics. Section 4 provides results for

validation and intercomparison with additional details given in supplementary material. Section 5 discusses the implications of these results for our research questions and the limitations of our study. Section 6 offers conclusions regarding the thematic performance of SL2P LAI, fCOVER and fAPAR over the sampled North American Forests and recommendations for future validation and SL2P improvements.

Table 2. Summary of thematic uncertainty assessments of SL2P products. All studies use in-situ PAI (regular print) or PAIe (italics) for reference values. A: accuracy. P: precision. U: uncertainty defined in Fernandes et al., 2014. ESU: elementary Sampling Unit. Land cover (LC) specified in Table 4.

Study	Region	land cover	#sites/ #ESUs	In-situ Range	FCOVER	LAI	FAPAR
Brown et al., 2019	United Kingdom	DBF	1/19	LAI:[1,4]		A 1.55 P 0.72 U -1.52	
Brown et al., 2021	United States of America	ENF	2/2	LAI:[0,6.5] FAPAR:[0,1]		A 0.0 P U 0.25	A 0.0 P U 0.05
Brown et al., 2021	United States of America	DBF	4/4	LAI:[0,6.5] FAPAR:[0,1]		A 0.32 P U 0.63	A -0.02 P U 0.09
Brown et al., 2021	United States of America	MF	3/3	LAI:[0,6.5] FAPAR:[0,1]		A 0.52 P U 0.91	A -0.05 P U 0.10
Brown et al., 2021	United States of America	DBF	2/2	LAI:[0,6.5] FAPAR:[0,1]		A 0.22 P U 0.68	A -0.01 P U 0.06
Djamai et al. 2018	Canada	CR	1/150	FCOVER: [0.5,0.92] LAI: [1,4.5]	A -0.02 P U 0.12	A -0.37 P U 0.98	
Hu et al. 2020	Southern Europe/ Kenya	DBF	6/19	FCOVER: [0.5,0.92] LAI: [1,4.5] FAPAR:[0.5,0.9]	A -0.10 P U 0.12	A -0.52 P U 0.61	A -0.10 P U 0.12
Hu et al. 2020	Southern Europe/ Kenya	CR	6/84	FCOVER: [0.1,1.0] LAI: [0.5,5.5] FAPAR:[0.2,0.95]	A -0.10 P U 0.18	A -0.39 P U 1.24	A -0.02 P U 0.14
Hu et al. 2020	Southern Europe/	GR	6/8	FCOVER: [0.05,0.75] LAI: [0.2,2.2]	A -0.05 P	A -0.19 P	A -0.03 P

	Kenya			FAPAR:[0.10,0.75]	U 0.17	U 0.42	U 0.39
Kganyago et al. 2020	South Africa	CR	1/65	LAI:[1.4,5.83]		A -2.15 P U 2.26	
Putzenlechner et al., 2019	Germany	MF	1	FAPAR:[0.91,0.99]			A -0.25 P U 0.24
Putzenlechner et al., 2019	Canada	DBF	1	FAPAR:[0.55,0.99]			A -0.07 P U 0.16
Putzenlechner et al., 2019	Costa Rica	DBF	1	FAPAR:[0.82,1]			A -0.32 P U 0.20

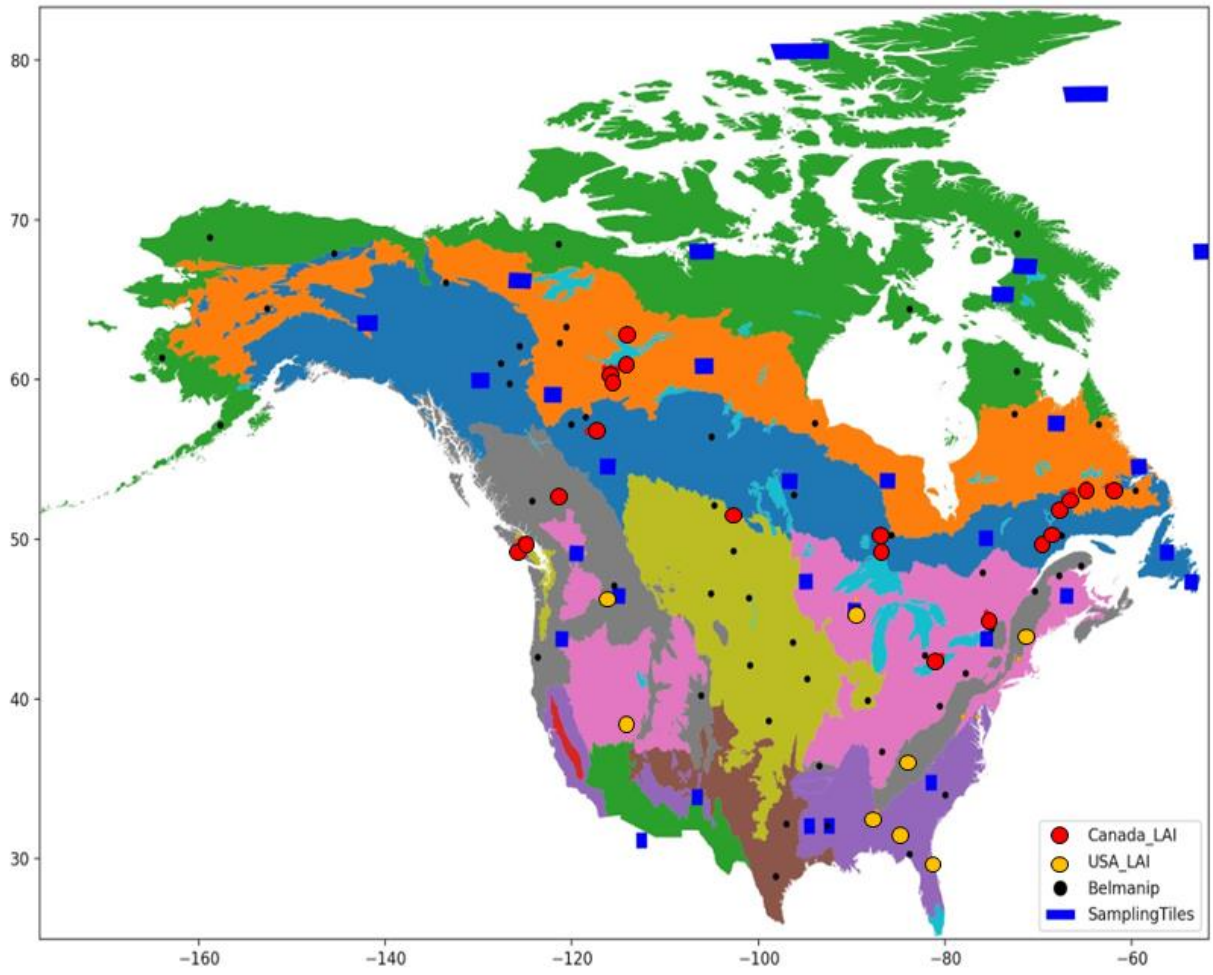

Figure 1. Location of intercomparison regions (blue rectangles) and in-situ reference measurement sites (red and yellow circles within North American Forest Ecological Regions. Global BELMANIP intercomparison sites are indicated as well (black circles).

2. Data Sets

2.1 Geospatial Datasets

Geospatial data were used for SL2P product generation, stratification of intercomparison, and product intercomparison (Table 3).

Table 3. Geospatial data sets.

Dataset	Description	Access	Reference
CGLSV1	333m 10d fAPAR at 10.15 Local Time, fCOVER and LAI	http://land.copernicus.eu/global/products/	Verger and Descals, 2022.
MERIT DEM	3 arc second Multi Error Removed Improved DEM	https://developers.google.com/earth-engine/datasets/	Yamazaki D., et. al. 2016
MCD15	500m 4d MODIS Collection 6 Leaf Area Index/FPAR	https://developers.google.com/earth-engine/datasets/catalog/MODIS_006_MCD15A3H	Myneni et al., 2015
MSI L2A	MSI Level 2A Bottom of atmosphere reflectance	https://developers.google.com/earth-engine/datasets/catalog/COPERNICUS_S2_SR	Copernicus Sentinel data 2019,2020
Forest Ecozones	North American Forests Primary Ecological Zones	http://www.cec.org/north-american-environmental-atlas/north-american-forests-2022/	Commission for Environmental Cooperation, 2022
NALC2015	30m North American Land Cover 2015	http://www.cec.org/north-american-environmental-atlas/land-cover-30m-2015-landsat-and-rapideye/	Commission for Environmental Cooperation, 2020

2.1.1 MERIT-DEM

MERIT-DEM is a 3 arc second resolution digital elevation model (DEM) produced by combining a number of available DEMs. The vertical uncertainty is <+/-9m over forested areas with slope <10% (Yamazaki D., et. al. 2015).

2.1.2 CEC Forest Ecozones

CEC Forest Ecozones is a polygon coverage of forest ecological zones for North America produced jointly by the Governments of Canada, United States of America and Mexico and published by the Council for Environmental Cooperation (CEC, 2022) (Figure 1). The map indicates 18 different primary forest ecological zones based on a combination of climate and potential vegetation classifications. The thematic uncertainty of this map is not given as it is a potential rather than actual geophysical dataset.

2.1.3 NALC2015

NALC2015 is a 30m resolution land cover map for North America circa 2015 with a 19 class legend (Table 4) (CEC, 2020). The land cover is nominally based on peak growing season satellite imagery from Landsat 5 and 8, as well as RapidEYE over the U.S.A., from 2015; with missing pixels replaced using the most recent valid year peak season estimate. The thematic uncertainty of products using the same monitoring system has been assessed over Canada with 79.9% correct labelling for all 19 classes and 83% correct labelling of forest classes (Latifovic et al. 2012). The spatial uncertainty of NALC2015 is less than 5m, 67.5% circular error probable. The NALC legend was translated to International Geosphere Biosphere Programme (IGBP) classes (Lambin and Geist, 2006) used to label the RM sites.

Table 4. NALC2015 land cover classes, IGBP Class acronym and forest land class designation. IGBP Classes: mixed forest (MF), deciduous broadleaf forest (DBF), evergreen needleleaf forest (ENF), grassland (GR), shrub (SH). evergreen broadleaf forest (EBF), barren land (BL (, cropland (CR), wetland (WL), urban (UB), water (WA), snow or ice (SI).

NALC2015 Class	IGBP Class	Forestland Class
Temperate or sub-polar needleleaf forest	ENF	Yes
Sub-polar taiga needleleaf forest	ENF	Yes
Tropical or sub-tropical broadleaf evergreen forest	EBF	Yes
Temperate or sub-polar broadleaf deciduous forest	DBF	Yes
Mixed forest	MF	Yes
Tropical or sub-tropical shrubland	SH	Yes
Temperate of sub-polar shrubland	SH	Yes

Tropical or sub-tropical grassland	GR	No
Tropical or sub-polar grassland	GR	No
Sub-polar or polar shrubland-lichen-moss	SH	No
Sub-polar or polar grassland-lichen-moss	GR	No
Sub-polar or polar barren-lichen-moss	GR	No
Wetland	WL	Yes
Cropland	CR	No
Barren lands	BL	No
Urban and built-up	UB	No
Water	WA	No
Snow/Ice	SI	No

2.1.4 MCD15

MCD15 corresponds to global 4-day composites of fAPAR and LAI gridded at 500m resolution. One valid retrieval based on the MODIS Version 6 fAPAR and LAI algorithm (Myneni et al., 2015) applied to MODIS on Terra and Aqua satellites is selected within each non-overlapping 4-day period. The thematic uncertainty of MCD15 over forests is reported in a number of studies (Table 5). Brown et al. 2020 report a root mean square difference (RMSD) between 0.48 to 1.05 for LAI and 0.09 to 0.14 for FAPAR for 547 samples at 18 sites across North America. Yan et al. (2016) report a maximum LAI (fAPAR) residual of +2/-1 LAI and +/-0.2 fAPAR for 50 samples with reference LAI ranging from 1.2 to 6 and fAPAR from 0.25 to 0.9. MCD15 underestimated LAI by between -0.14 (Brown et al. 2020) and -0.41 (Fuster et al. 2020) over ENF and by -1.47 for MF (ZJin et al., 2017). The geolocation uncertainty of MCD15 is better than 53m RMSE (Lin et al., 2019) although the projected instantaneous field of view of measurements can vary by a factor of 4.83 across track (2.01 along track) for extreme view angles over flat terrain (Wolfe et al., 1998).

Table 5. Review of thematic uncertainty assessments of MCD15 version 6 products over forests. A: accuracy. P: precision. U: uncertainty defined in Fernandes et al., 2014. Land cover (LC) specified in Table 4.

Study	Region	LC	#sam.	In-situ Range	LAI	FAPAR
Brown et al., 2020	USA	ENF	122		A -0.14 P U 0.42	A 0.0 P U 0.09
Brown et al., 2020	USA	EBF	81		A 0.54 P U 0.77	A 0.0 P U 0.10
Brown et al., 2020	USA	DBF	158		A -0.05 P U 0.90	A -0.01 P U 0.12
Brown et al., 2020	USA	MF	86		A -0.08 P U 0.96	A -0.06 P U 0.13
Brown et al., 2020	USA	WL	81		A -0.10 P U 0.72	A -0.02 P U 0.11
Yan et al. 2016	Global	MF	50	LAI: [1,2.6] FAPAR:[0.25,0.95]	A P U [-1,+2]	A P U [-0.2,0.2]
Nestola et al. 2017	Italy	BF				A 0.003 P U 0.06
Fuster et al. 2020	Spain	ENF	800	FCOVER: 0.18,0.4] FAPAR: [0.2:0.5] LAI:[0.6,1.6]	A -0.41 P U 0.48	A 0.09 P U 0.10
Jin et al. 2017.	China	MF	286	LAI:[1,8]	A -1.47 P U 2.29	

2.1.5 CGLSV1

CGLSV1 corresponds to CGLS Ocean Land Colour Imager (OLCI) Version 1.1 fAPAR, fCOVER and LAI products gridded at 300m resolution for non-overlapping 10-day periods (Verger and Descals, 2020). CGLSV1 is a Level 4 product in that temporal interpolation using both current and historical retrievals for a mapped pixel are applied. Here, only composites without interpolated products are used. The input

Level 2 fAPAR and LAI products are derived by a neural network calibrated to relate OLCI BRF to CGLS ProbaV Products (PBV 300m V1 v1.0, Baret et al. 2016) that in turn are estimated using a weighting of corresponding MCD15 Version 5 (Yang et al., 2006) and CYCLOPES V3.1 (Baret et al., 2007) products; with the CYCLOPES V3.1 weighing transitioning from >80% for LAI<1 to <20% for LAI>2. Input Level 2 fCOVER is derived using a fixed logarithmic relationship between fCOVER and LAI. In terms of thematic uncertainty, Brown et al. 2020 report an uncertainty of 0.25 to 0.91 for LAI and 0.05 to 0.09 for FAPAR for 538 samples at 18 sites across North America. Over the same sites, Fuster et al. (2020) reported much larger residuals (often exceeding +/-1 LAI and +/-0.1 fAPAR) but did not use spatial weighting with ancillary layers when upscaling in-situ RM. The spatial uncertainty of CGLS products is generally well below 100m over flat terrain (http://proba-v.vgt.vito.be/en/quality/platform-status-information/geolocation-accuracy). Information regarding the variation of the PIFOV with view geometry is not available but is likely much smaller than MCD15 products as the Operational Line Imager uses multiple oriented cameras for cross track sampling.

Table 6. Review of thematic uncertainty assessments of CGLS products. A: accuracy. P: precision. U: uncertainty defined in Fernandes et al., 2014. ESU: elementary Sampling Unit. Land cover (LC) specified in Table 4.

Study	Region	LC	#ESU	In-situ Range	FCOVER	LAI	FAPAR
Brown et al., 2020	USA	ENF	111			A 0.0 P U 0.25	A 0.0 P U 0.05
Brown et al., 2020	USA	EBF	80			A 0.2 P U 0.47	A -0.02 P U 0.07
Brown et al., 2020	USA	DBF	174			A 0.32 P U 0.63	A -0.02 P U 0.09
Brown et al., 2020	USA	MF	94			A 0.52 P U 0.91	A -0.05 P U 0.10
Brown et al., 2020	USA	WL	79			A 0.22 P U 0.68	A -0.01 P U 0.06
Fuster et al. 2020	Global	ENF	175	FCOVER: 0.18,0.4] FAPAR: [0.2:0.5] LAI:[0.6,1.6]	A -0.02 P U 0.04	A -0.35 P U 0.38	A 0.037 P U 0.05

Zhao et al. 2020	China	MF	286	LAI:[2,8]		A -0.54 P U 1.21	

2.1.6 MSI L2A

MSI L2A data corresponds to level 2A bottom-of-atmosphere BRF processed from MSI top-of-atmosphere L1B products by ESA from the MSI on S2A or S2B satellites, using version 2.10 or higher of the SEN2COR algorithm (Müller-Wilm, 2018). The thematic uncertainty for recognition of clear pixels over land and water was 98% and the radiometric uncertainty was better than 0.005 + 0.05BRF for flat surfaces (Clerc et al. 2020; Doxani et al., 2018); although the latter could increase substantially over terrain with adjacent slopes exceeding 10° (Djamai and Fernandes, 2019). The spatial uncertainty is less than 12.5m CE95 (95 percentile of the circular error) (Gascon et al. 2017). The full width half maximum point spread function ranges from 22m for the 10m Band 4, to 33.40 m and 39.1m for Band 5 and Band 11 respectively (Radoux et al., 2016).

2.2 In-Situ Reference Measurements

In-situ reference measurements (RM) spanning 2019 and 2020 were acquired from the Ground-Based Observations for Validation (GBOV) component of the CGLS (Brown et al. 2021) and by the authors at Canada Centre for Remote Sensing (CCRS) (Table 7).

2.2.1 GBOV

fIPAR, fCOVER and LAI RM were derived from Digital Hemispherical Photographs (DHPs) for 142 Elementary Sampling Units (ESUs) at 14 sites within the National Ecological Observatory Network (Kao et al. 2012) forest or shrubland sites in North America. GBOV defines fIPAR as the black-sky PAR intercepted by overstory and understory vegetation at 10:00 local time and LAI as the one-sided leaf area per unit ground surface area a Brown et al. (2021). In fact, the GBOV LAI actually corresponds to half the total plant area per unit horizontal ground area (PAI) (L. Brown personal communication).

At each site, three 20m by 20m square ESUs, located within 1km of NEON tower locations, were sampled bi-weekly from leaf-out to senescence. In each ESU, 12 co-located upward and downward looking DHP images were acquired with 4m spacing in North-South and East-West transects through the plot centre using 36.3MPixel Nikon D810 cameras with Nikon 16m Fisheye lenses giving a 180° diagonal field of view (FOV) (Figure 2). The ESU centre location was determined within 1m 90% circular error probable (C.E.P.). Five sites included additional intensive sampling dates at up to 22 additional ESUs within 1km of the tower.

DHPs were visually quality controlled by GBOV, masked to remove the field operator, and processed using software developed by GBOV to derive measurement estimates and associated 1 standard deviation (σ) uncertainties. PAI was estimated using the gap fraction at 57.5° zenith (Lang and Yueqin, 1986). The effective PAI (PAIe), defined as the PAI required to match the observed gap fraction assuming a canopy of opaque randomly distributed foliage, was also estimated (Warren-Wilson, 1963). PAI and PAIe 1σ uncertainties were estimated as the Euclidean sum of the standard error of the measured variable over all DHPs at a plot and the 1σ uncertainty due to instrument levelling.

2.2.2 CCRS

fIPAR, fCOVER and PAI RM were derived from DHPs acquired for 133 ESUs in Natural Resources Canada's Cumulative Effects study sites across Canada (Figure 1). ESUs were located within the dominant land cover types at each site with replication where logistics permitted. For each ESU, seven co-located upward and downward DHP images were acquired every 5m along two parallel transects spaced 15m apart (Figure 2) using 45.7 MPixel Nikon D850 cameras with a Nikon 8mm Fisheye lens (https://www.nikon.com/) giving a 180° FOV in all directions. The ESU centre was located to within 5m 90% C.E.P. in addition, the IGBP land cover class and the approximate surface cover fraction of bryophyte, lichen, mineral soil or litter was noted.

DHPs for each ESU sampling date were quality controlled visually, contrast enhanced using ViewNXi software (https://en.nikon.ca/nikon-products/product/imaging-software/viewnx-i.html), masked to remove the field operator, and processed using CANEYE V6.45 (https://www6.paca.inrae.fr/can-eye/Download/) to derive measurement estimates as well as PAIe and associated 1σ uncertainties

using the same approach as GBOV. CANEYE also provides a second PAIe and PAI estimate, used here, that minimises the difference of the observed gap fraction for each position in the hemisphere and the modelled gap fraction given the estimates PAIe under the constraint that the GBOV estimate is also matched to within measurement uncertainty of gap fraction at 57.5° zenith. Agreement of the GBOV and CANEYE algorithms is actually a necessary condition if indeed the canopy was sufficiently sampled and DHPs were adequately processed. As part of the CCRS protocol, ESU measurements where these two approaches differed in excess of their average standard error were processed after further quality control and enhancement. This approach also ensured a level of consistency between GBOV and CCRS RM.

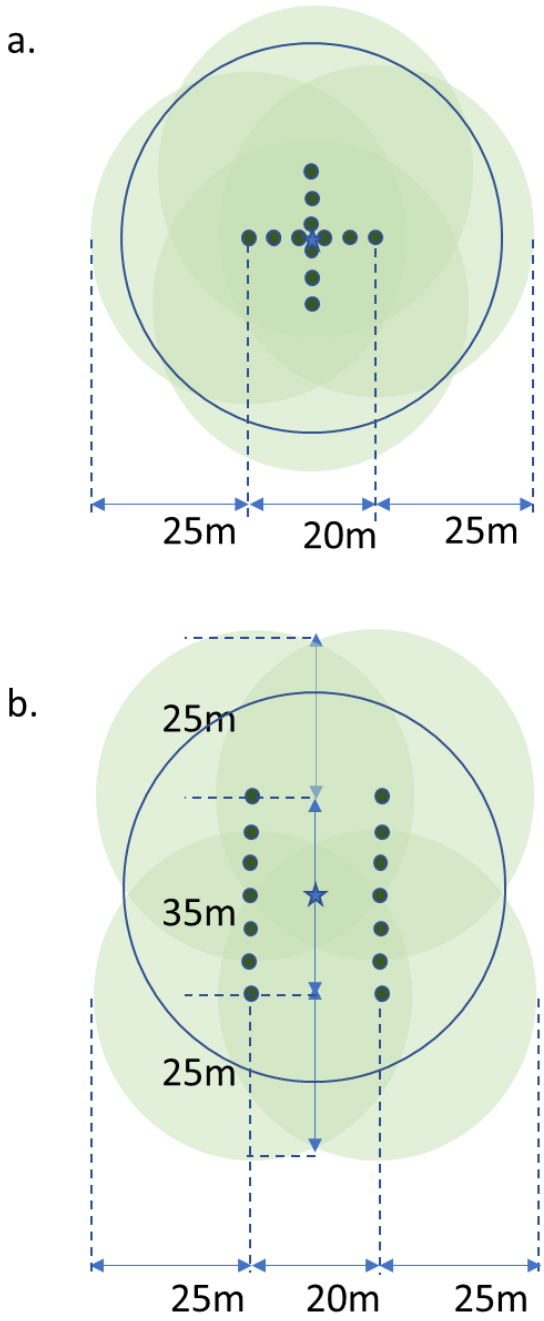

Figure 2. Schematic of a. NEON and b. CCRS Elementary Sampling Unit (ESU) design. Star: ESU centre; dark green solid circles: understory DHP 60° FOV for 50cm canopy; light blue solid circles: overstory DHP 60° FOV for 20m tall canopy; blue circle: 30m radius SL2P product sampling buffer.

Table 7. In-situ sites. ESU: Elementary Sampling Unit.

Site	Ecoregion	IGBP Class	Lat. °N	Long. °E	Elev. (m a.s.l.)	Date Start	Date End	#ESU	Network
Bartlett Exp. Forest	Northern Forests	MF	44.06	-71.28	232	2019-05-13	2020-10-12	3	GBOV
Blandy Exp. Farm	Eastern Temperate Forests	DBF	39.08	-77.95	183	2019-03-26	2020-10-14	22	GBOV
Dead Lake	Eastern Temperate Forests	DBF	32.53	-87.8	22	2019-03-13	2020-08-07	22	GBOV
Disney Wilderness Preserve	Northwestern Forested Mountains	MF	42.53	-72.18	15	2019-01-03	2020-12-15	24	GBOV
Geraldton	Northern Forests	ENF	31.19	-84.47	348	2020-07-15	2020-07-21	56	CCRS
Guanica Forest	Tropical Dry Forests	ENF	40.04	-105.55	143	2019-01-07	2020-12-16	3	GBOV
Harvard Forest	Eastern Temperate Forests	MF	35.96	-84.28	351	2019-05-08	2020-10-06	3	GBOV
Hay River	Northern Forests	ENF	60.42	-116.35	165	2019-09-05	2019-09-07	28	CCRS
Jones Ecological Research Ctr.	Eastern Temperate Forests	ENF	29.69	-81.99	44	2019-01-10	2020-12-08	24	GBOV
Joronarda	North American Deserts	SH	32.59	-106.84	36	2019-01-10	2020-12-08	3	GBOV
Labrador	Taiga	DBF	45.50	-89.58	12	2019-07-24	2019-07-31	7	CCRS
Mer Bleu	Eastern Temperate Forests	ENF	32.95	-87.39	86	2019-09-18	2019-09-18	3	CCRS
Moab	Northwestern Forests Mountains	SH	38.25	-109.38	1799	2019-01-10	2020-12-08	3	GBOV
MtPolley	Marine West Coast Forest	SH	28.12	-81.43	917	2019-08-12	2019-08-15	6	CCRS
Nova Scotia	Northern Forests	SH	38.24	-109.38	34	2021-06-09	2021-08-27	7	CCRS

Oak Ridge	Eastern Temperate Forests	SH	40.17	-112.45	334	2019-04-16	2020-10-24	3	GBOV
Onaqui Ault	Northwestern Forested Mountains	SH	31.91	-110.83	1685	2019-03-20	2020-08-26	3	GBOV
Ordway Swisher Biological Stn.	Northern Forests	EBF	17.96	-66.86	45	2019-01-28	2020-11-13	3	GBOV
Peace River	Northern Forests	ENF	60.42	-116.35	330	2019-08-12	2019-08-12	9	CCRS
Santa Rita	Temperate Sierras	MF	50.59	-68.78	983	2019-03-04	2020-10-06	3	GBOV
Smithsonian Conservation Biology Inst.	Eastern Temperate Forests	ENF	45.40	-75.56	361	2019-05-21	2020-10-15	3	GBOV
Talladega National Forest	Northwestern Forested Mountains	ENF	52.55	-121.66	135	2019-03-19	2020-07-01	3	GBOV
Turkey Point	Eastern Temperate Forests	DBF	56.74	-118.34	222	2019-06-25	2019-06-27	4	CCRS
University Notre Dame Conservation	Eastern Temperate Forests	DBF	42.63	-80.55	518	2019-05-08	2020-09-30	23	GBOV
Vancouver Island	Marine West Coast Forest	MF	49.96	-125.57	50	2019-08-09	2019-08-10	7	CCRS
Yellowknife	Northern Forests	ENF	62.55	-114.00	206	2019-08-09	2019-08-12	6	CCRS

3. Methods

3.1 Reference Measurements

RM were uploaded to GEE as feature collections (Fernandes et al., 2022). PAIe, PAI, fIPAR and fCOVER were converted to LAIe, LAI, fAPAR and green fCOVER by multiplying the measured value by woody area to total area ratios given in Brown et al. (2021) for the overstory and 0.05 (+/-0.025 1σ) for the understory. The understory value was selected assuming herbaceous and shrub understory cover have non-zero woody to total area ratio but typically less than trees due to absence of trunks. Total LAIe, LAI, fAPAR and fCOVER were estimated by combining understory and overstory values as in Brown et al. (2021). Clumping was calculated as the ratio of total LAIe to total LAI. A clumping of one corresponds to a canopy with random foliage locations while lower values indicate foliage that has increasing spatial clumping.

The 1σ uncertainty of overstory or understory components of each RM was estimated as the Euclidean sum of the 1σ uncertainties due to levelling error, sampling variability, the applied woody to total area ratio, and for LAI, a 0.025 1σ uncertainty for clumping; the latter not accounting for systematic theoretical biases in estimating clumping that are as yet not well quantified (Leblanc et al., 2006; Ryu et al., 2010). The 1σ uncertainty of the corresponding total RM value was estimated as the Euclidean sum of the constituent understory and overstory 1σ uncertainties weighted by their proportion of the total RM.

3.2 Validation

The LEAF-Toolbox implementation of SL2P was used to map LAIe, LAI, fAPAR and fCOVER and associated quality control and theoretical precision layers at 20m resolution for clear sky land pixels whose centroid fell within a 30m radius of the centre of each ESU and +/-7d interval of each RM. Retrievals flagged by SL2P as low quality were masked from further processing. SL2P applies separate non-linear regressions to estimate fAPAR, fCOVER, LAI and associated theoretical precision given a MSI L2a BRF and associated acquisition geometry. Each non-linear regression is calibrated using a database of 42,378 simulated BRFs with associated canopy variables produced by applying the turbid homogeneous (i.e. clumping=1)

PROSAILH radiative transfer model (Verheof et al., 2007) to a sample of canopy parameters draw from globally representative priors.

The SL2P implementation in SNAP was not used as two bugs were identified in the MATLAB libraries provided to SNAP and subsequently verified by M. Weiss (personal communication): i) incorrect truncation of the prior probability distributions used to specify realizations of simulated canopies for calibration of the neural network used to estimate product values, ii) a coding error in the algorithm used to flag out of domain retrievals that significantly overestimated the frequency of poor quality retrievals. To understand the impact of these bugs for current users of SNAP, SNAP and LEAF-Toolbox products were compared over the validation site used in Djamai et al. (2019).

The +/7d interval for matches ensured at least three MSI acquisitions for each sample date given the <5d revisit of Sentinel 2a and 2b MSI imagers. Temporal variability of SL2P matches during the start and end of season or during rapid disturbance or drought and SL2P uncertainty due to geolocation or atmospheric correction errors were reduced by discarding dates where the majority of samples exceeded the 50%ile absolute residual of all matched pixels for the 15d period at a given ESU.

For each variable, population statistics for U, P and uncertainty agreement ratio (UAR) and coefficient of determination (r^2) were computed as in Brown et al. (2021); with U and P corresponding to the population root mean square difference and bias respectively. Population A was not computed since it varies systematically with the RM value. The 1σ uncertainty of the mean SL2P estimate for a given match-up was modelled as the Euclidean sum of the mean SL2P theoretical and the standard error of the matching SL2P samples.

Good practice requires reporting thematic performance as a function of the RM value to allow for comparisons of validation results across studies with different sampling distributions (Fernandes et al., 2014; Doxani et al. 2018; Brown et al. 2021). To do so, third order polynomial weighted least squares regression was fitted to quantities based on residuals between the mean of matching SL2P product pixels and RM values were used to model A , P and U. For A (U) the residual (absolute residual) between SL2P estimates and RM was regressed against the RM. For P, the SL2P estimates were first corrected by adding the modelled A followed by regressing the absolute residuals between the corrected SL2P

estimates and RM against the RM. The expected conditional value and +/-95%ile confidence intervals of each regression were computed using statsmodel version 01.3 (https://www.statsmodels.org/stable/index.html).

3.3 Intercomparison

Product intercomparison should be performed over replicate regions sampled within unique land surface conditions (Fernandes et al. 2014). The BELMANIP2 sampling design was developed to sample regions based on strata representative of global biomes, land cover and phenology together with the constraint that sample regions minimise conditions not relevant to the stratum and have relatively flat terrain (Weiss et al., 2014). . The last condition reflects the fact that complex terrain can result in both radiometric and geolocation uncertainty that can mask differences in the retrieval algorithms. BELMANIP2 was not used here for three reasons: i) it misses two North American forest ecozones ii) even within a forest ecozone the regions are located to match the expected distribution of all land cover rather than only forest cover and iii) it does not consider the number of valid product intercomparisons available within forested regions. Instead, since our study only considers North American forests, we relied on the North American forest ecozone map to stratify by geographic location, forest type, and phenology. Sample regions were restricted to 100km x 100km Military Grid Reference System (MGRS) tiles (Defence Mapping Agency, 1990) since they offer a global equal area grid and because S2 L2a products are formatted using these tiles.

MGRS tiles were scored using the product of four relative criteria scores to select tiles that maximise potential valid intercomparisons. Each relative criteria score corresponds to a raw criteria score (Table 8) divided by the sum of the same raw score over all overlapping tiles. The product of relative scores ensured that the selected MGRS tile would not rank low on any one of the relative scores. For each forest ecozone, all MGRS tiles with at least 50% overlap with the ecozone were scored and the two tiles with the highest score selected.

Table 8. Raw criteria scores for selecting MGRS tiles.

Name	Definition	Inputs
Forest Area	Average forest area within 3x3 MCDIS pixel footprints.	NALC2015
Land Area	Average land area within 3x3 MCDIS pixel footprints.	NALC2015
Elevation Deviation	1 of MERIT elevation within 3x3 MCD15 pixel footprints.	MERIT DEM
Vegetation Homogeneity	Growing season average of 1 SL2P NDVI within a 3x3 MCDIS pixel footprints	MSI L2A Products April-September, 2019
Clear Sky Count	Number of dates with >90% coverage of clear sky MSDI L2a retrievals in each 3x3 MCDIS pixel footprint.	MSI L2A Products April-September, 2019

Match-ups were extracted for each MSI L2a BRF product acquired during 2019 over selected MGRS tile. For each non-overlapping 3x3 (for MODIS) or 5x5 (for CGLS) coarse resolution product pixel, areas labelled as either water in the L2a scene classification mask, water or built-up in the NALC2015 land cover, or L2a normalised difference vegetation index<0.1, were assigned biophysical parameter estimates of zero. SL2P was applied to other areas in the footprint using the corresponding 20m L2a BRF product to estimate canopy biophysical parameters and associated theoretical. Intercomparisons for a 3x3 pixel footprint were considered valid if at least 90% of the footprint area was mapped with valid SL2P retrievals or zero values and with 100% coverage of valid highest quality coarse resolution product retrievals.

4. Results

4.1 Verification

Comparisons of SNAP and LEAF-Toolbox implementations of SL2P indicated differences in both LAI and Quality Masks. SNAP overestimates (underestimates) LEAF-Toolbox for LAI>4 (LAI< 2) (compare Figure 3a. to Figure 3b.). SNAP also typically designates >50% of SL2P retrievals as invalid due to being 'Out of Domain' of the calibration dataset in comparison to only ~10% for SL2P (compare Figure 3c. to Figure 3d). Further, SNAP maps all L2a reflectance measurements including clouds while SL2P only maps clear sky land.

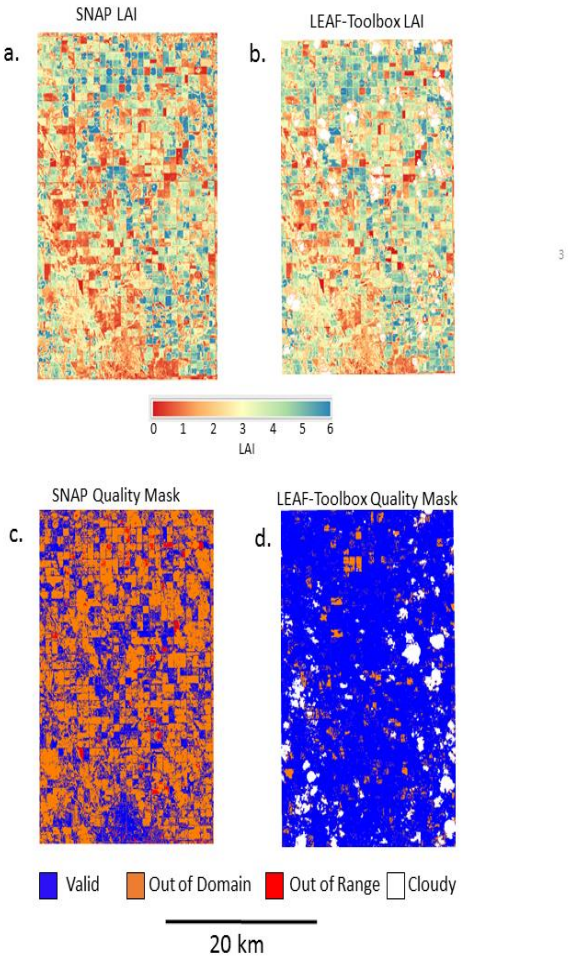

Figure 3. Comparison ofSL2P implemented in SNAP LAI and quality mask (a. and c.) to LEAF-Toolbox LAI and quality mask (b. and d.) for the agricultural region reported in Djamai et al. (2019).

4.2 Sampled SL2P and RM Estimates

On average, 8.07 (range [6.5,28]) matching SL2P pixels were found over each of 1107 RM samples of LAIe, LAI, fCOVER and fAPAR (Table 9). RM values spanned 0.01 to 7.41 for LAI and 0.002 to 0.95 for both fAPAR and fCOVER (Figure 4). The modal LAI value for MF and DBF was ~4.5 although the DBF sites had secondary mode of ~1.5 due to the inclusion of early season NEON sampling. ENF sites had a lower modal LAI than other forests (~1.5) due to the northern latitude CCRS sites. Closed SHB sites showed a relatively uniform distribution of LAI between ~2-3 while open SHB sites had a narrow mode at ~0.5 LAI.

fAPAR and fCOVER RM were almost linearly related as expected since both are weighted gap fraction estimates from the same DHP samples. Both quantities were logarithmically related to LAI as also expected from the relationship between gap fraction and LAI (Monteith and Unsworth, 1997). Except for shrublands, where clumping was always near 1, there was no clear relationship between clumping and land cover; although clumping was generally lower for CCRS versus NEON sites (Figure 4).

The univariate and bi-variate distributions of SL2P estimates (Figure 5) were similar to their RM counterparts but with somewhat greater spread and stronger linear relationships between fAPAR and fCOVER and logarithmic relationships between these variables and LAI. In contrast to the RM distributions, there was no visible distinction in bivariate distributions of SL2P products between CCRS and NEON sites.

Table 9. Summary of validation samples.

Site	#sam.	Median #matches	Median LAI	Median clumping	WAI to PAI ratio	WAI to PAI ratio stdev
Bartlett Experimental Forest	58	16	5.03	0.74	0.18	0.11
Blandy Experimental Farm	85	28	3.42	0.79	0.24	0.1
Dead Lake	66	10	4.67	0.74	0.24	0.1
Disney Wilderness Preserve	66	14	0.60	0.96	0.05	0.05
Geraldton	55	14	2.514	0.57	0.22	0.11
Guanica Forest	104	14	2.6825	0.67	0.16	0.11
Harvard Forest	55	14	1.80	0.75	0.18	0.11
Hay River	28	8	4.62	0.57	0.16	0.11
Jones Ecological Research Center	28	18	2.36	0.75	0.16	0.11
Joronarda	92	28	0.02	0.96	0.05	0.05
Labrador	36	6.5	0.86	0.59	0.16	0.11
Mer Bleu	6	24	3.56	0.58	0.16	0.11
Moab	3	8	0.02	1	0.05	0.05
MtPolley	11	16	4.07	0.61	0.25	0.11
Nova Scotia	6	14	4.83	0.55	0.24	0.11

Oak Ridge	28	24	4.62	0.76	0.18	0.11
Onaqui Ault	49	16	0.05	0.99	0.05	0.05
Ordway Swisher Biological Station	27	20	1.01	0.69	0.16	0.11
Peace River	73	13	1.51	0.62	0.18	0.11
Santa Rita	9	14	0.08	0.95	0.05	0.05
Smithsonian Conservation Biology Institute	66	16	5.27	0.65	0.18	0.11
Talladega National Forest	51	14	3.46	0.71	0.16	0.11
Turkey Point	42	13	2.53	0.58	0.24	0.11
University Notre Dame Conservation	4	20	4.45	0.69	0.18	0.11
Vancouver Island	74	24	3.24	0.52	0.16	0.11
Yellowknife	7	13.5	0.21	0.67	0.23	0.11

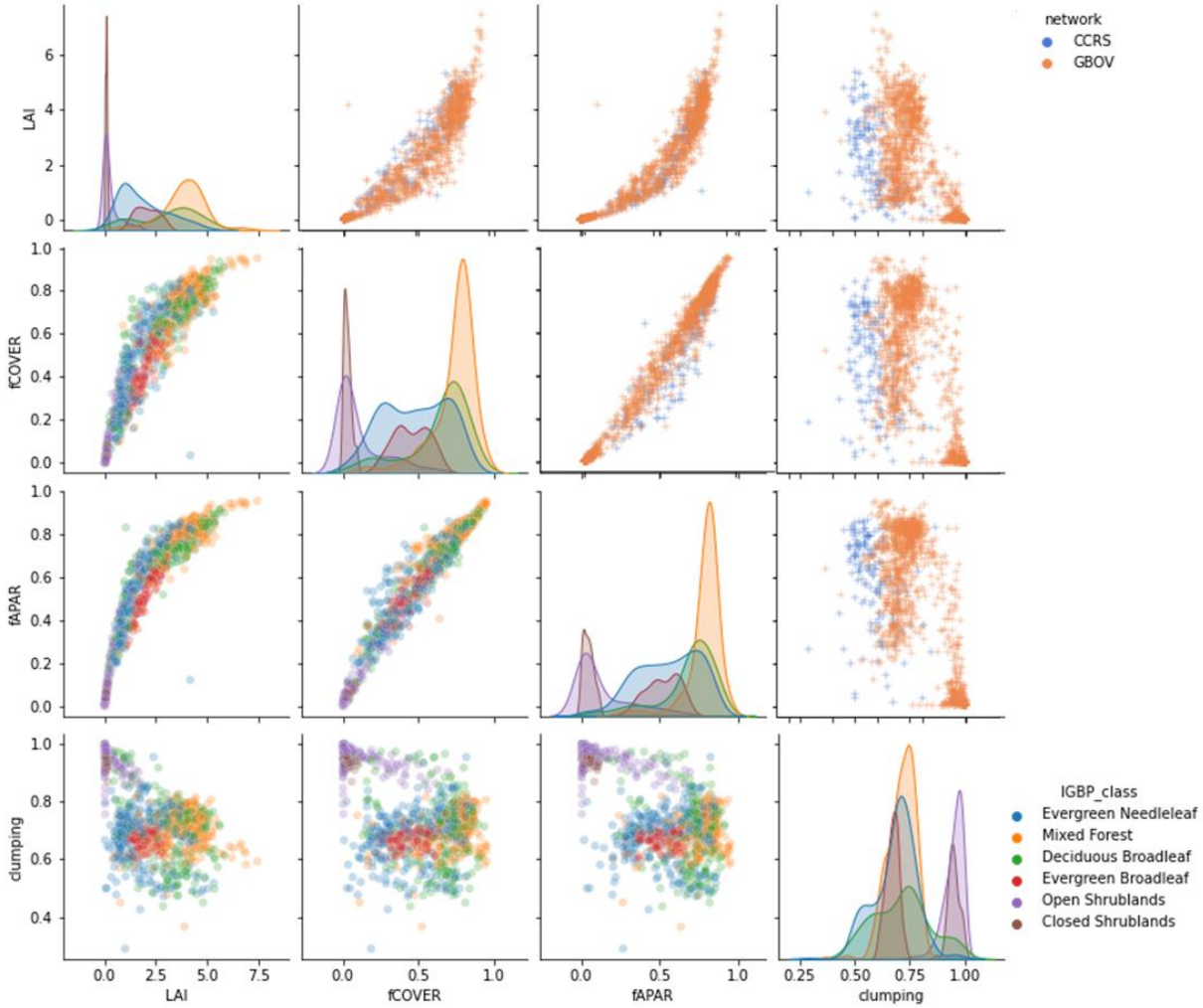

Figure 4. RM distributions by measurement network (upper diagonal figures) and IGBP land cover class (diagonal and lower diagonal figures).

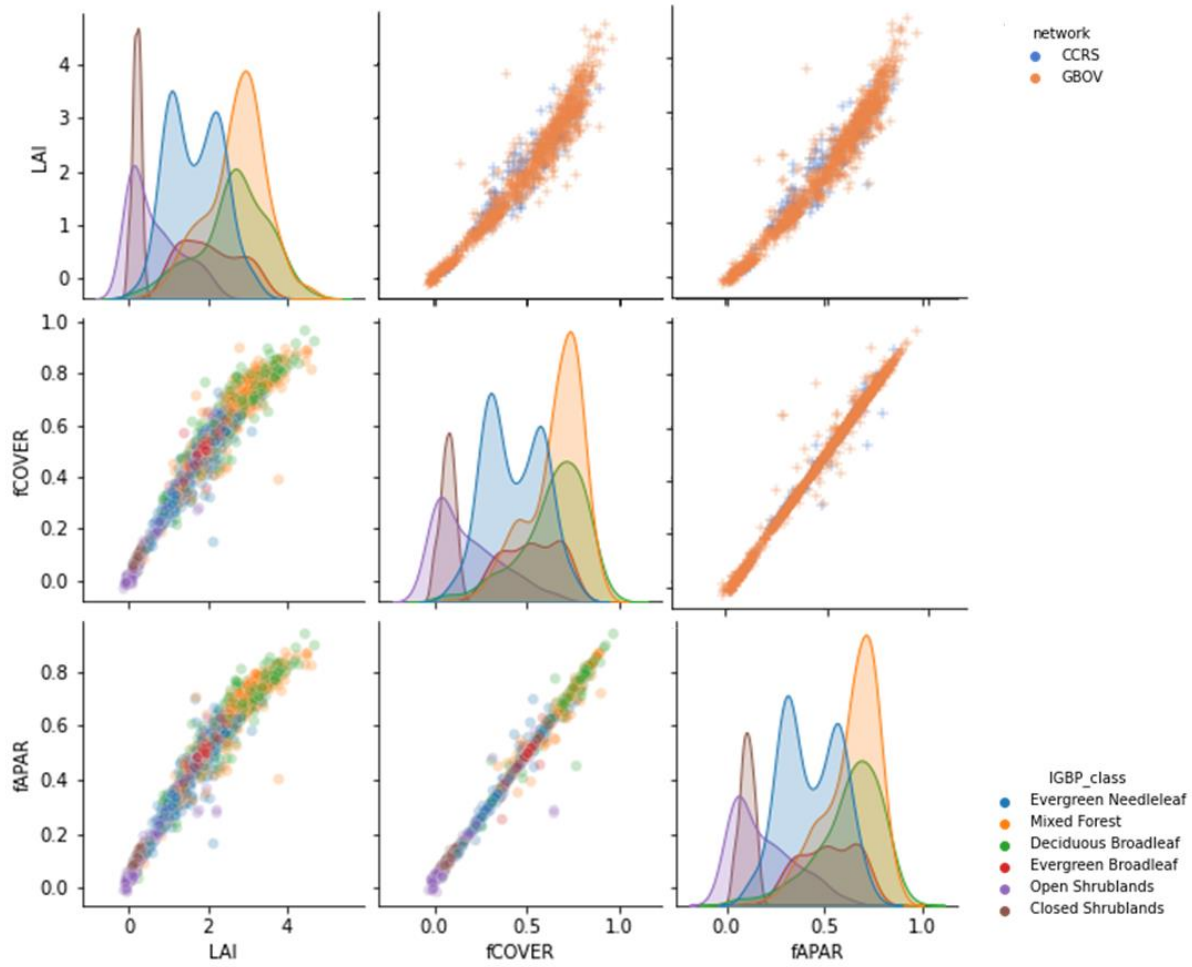

Figure 5. SL2P distributions by measurement network (upper diagonal figures) and IGBP land cover class (diagonal and lower diagonal figures).

4.3 Comparisons of RM and SL2P

4.3.1 Population Level Statistics

Scatter plots of SL2P versus RM LAIe (Figure 6a) and LAI (FIgure6b) indicate relatively linear relationships (r^2~0.65) with U and UAR of 0.68 and 58% respectively for LAIe and 0.99 and 48% respectively for LAI. LAIe was consistently overestimated with a modest bias of 0.33. LAI was relatively unbiased for LAI<2 and underestimate for LAI>2 so the population level LAI bias of -0.38 was not representative of local performance. Both fCOVER and fAPAR exhibited relatively linear relationships (r^2>=0.7) but fAPAR had lower slightly lower A than fCOVER (-0.07 versus -0.02) that translated into a lower UAR (31% versus 37%) even though U for both was ~0.15.

Qualitatively, there was no evidence of systematic differences in residuals when comparing CCRS and GBOV network comparison for the same land cover and RM value (Figure 6). Quantitative tests were not performed due to the imbalance of sample sizes between networks. In terms of land cover classes, for all variables the closed SHB were typically estimated with low uncertainty (e.g. <0.5 LAI, <0.05 fAPAR and fCOVER) while open SHB tend to be overestimated (between 0.5 LAI to 1 LAI and 0.05 and 0.2 fAPAR and fCOVER). Otherwise, the forest cover classes tended to correspond to a single bivariate distribution for either LAIe or LAI but showed larger fAPAR underestimation of MF and ENF in comparison to DBF or EBF.

The RM measurement uncertainty was typically on the order of +/-1 unit for LAIe and LAI and +/-0.05 units for fAPAR and fCOVER (Figure 7). SL2P LAI theoretical uncertainty for a single retrieval was also on the order of +/-1 unit but SL2P fAPAR and fCOVER theoretical uncertainties are only ~+/-0.025 unit; much less than for LAI even if we increase the fAPAR and fCOVER uncertainties by a factor of 4 given the relationship between SL2P LAI and these quantities (Figure 5).

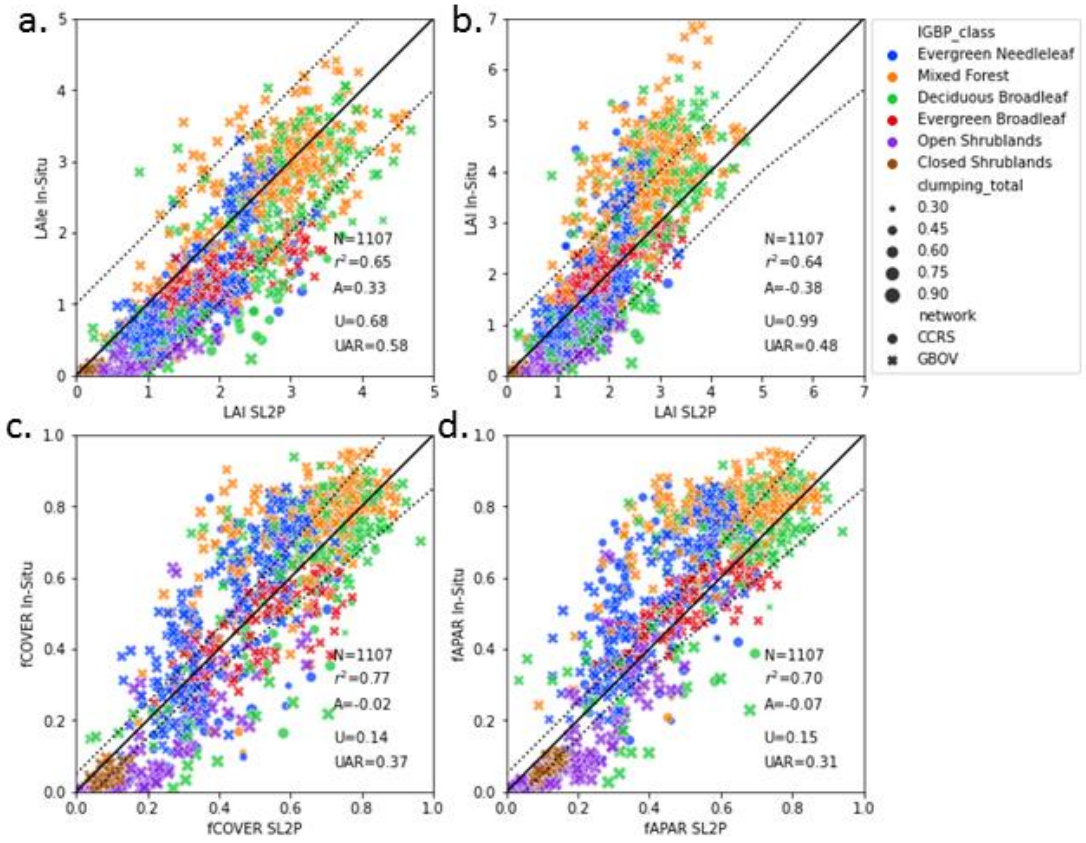

Figure 6. Scatter plots of mean SL2P estimates versus matching RM for each variable together with population validation metrics. Symbol shape indicates network, symbol colour indicates IGBP class and symbol size indicates clumping index. Dashed lines bound target user requirement around solid 1:1 line.

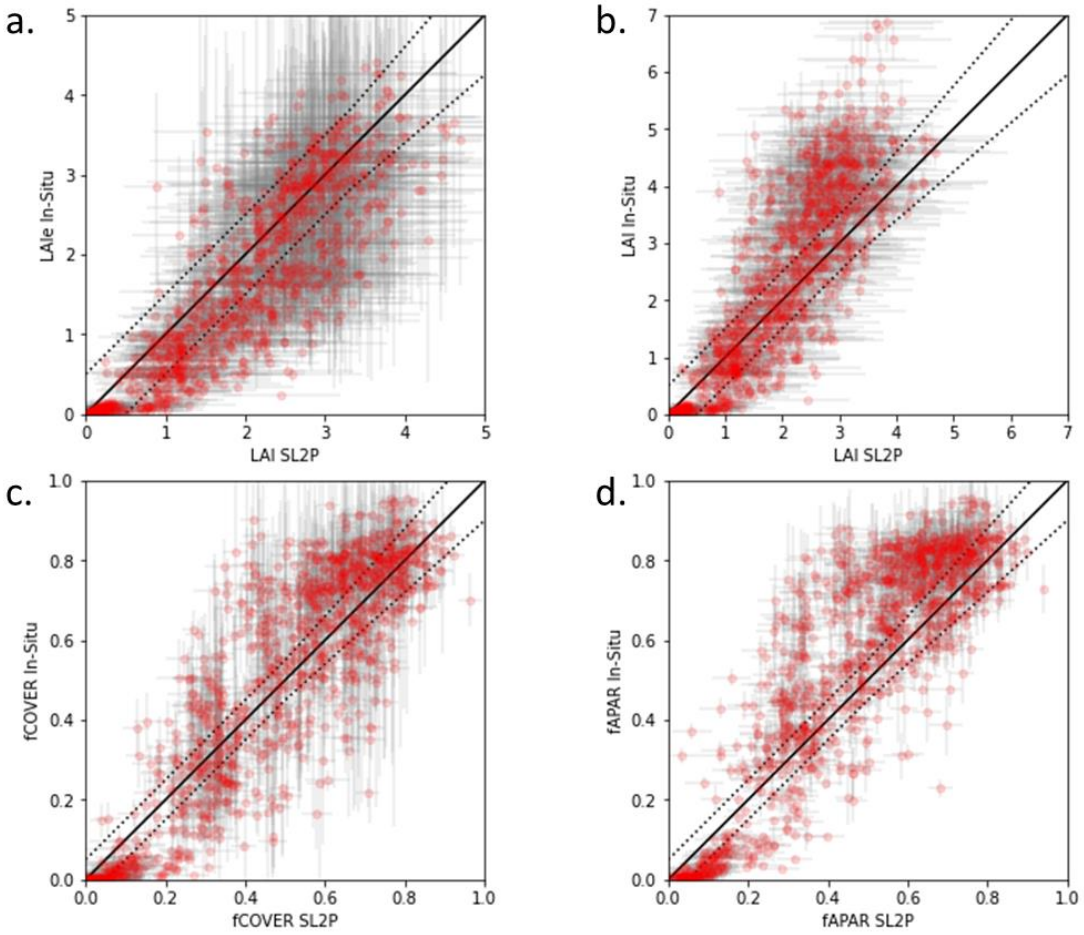

Figure7. Scatter plots of mean SL2P estimates versus matching RM values for each canopy variable together with 1σ uncertainty estimates. Dashed lines bound target user requirement around solid 1:1 line.

4.3.2 Accuracy, Precision and Uncertainty as a Function of RM Value

SL2P LAI estimated RM LAIe with bias (A) decreasing from 0.5 LAI at LAI~0 to -0.5 LAI at LAI~4 (Figure 8a.). However when compared to RM LAI, SL2P LAI was nearly unbiased (for LAI<2) but increasingly underestimated larger RM LAI; reaching an underestimate of -3 LAI units at LAI 6 (Figure 8b). In contrast the precision of SL2P LAIe and LAI was approximately ~0.5 LAI units for all levels of LAI. As a result, uncertainty of SL2P LAI as an estimate of RM LAIe was within target requirements for LAIe but exceeded LAI target requirements for LAI>3.

SL2P estimated RM fCOVER and fAPAR with an bias (A) of ~0.1 for the lowest RM values, to ~0 for mid-range RM values (~0.3 fCOVER and ~0.5fAPAR) and ~-0.15 for high (>0.8) RM values (Figure 8c. and 8d).

SL2P fCOVER and fAPAR precision was relatively constant ranging from ~0.05 at extreme RM values to ~0.1 for mid range RM values. For both fCOVER and fAPAR, the combination of relatively constant precision and changing accuracy resulted in greater uncertainty at low and high RM values; although uncertainty was typically between 0.08 and 0.15 for all retrievals.

The 95% confidence intervals of the A, P and U model fits were narrow for fAPAR and fCOVER (<+/-0.05) and for LAI<5 (<0.2) but was wider for high (>3) LAIe and (>5) LAI due to the increased non-linearity and decreased sample density. However, in these latter cases the magnitude of both A and U also increased so the A, P and U model confidence intervals were proportionally relatively constant in magnitude when compared to corresponding regression line magnitudes.

For all variables, the relationship between clumping and A was weak and non-monotonic (Figure 9). The weak relationship spanning our entire sample follows since, for all parameters, A was correlated to the RM magnitude (Figure 8) which in turn was not correlated to clumping but network (Figure 5). However, both P and U error decreased as clumping index increased in a relatively linear manner as evidenced by Pearson correlation coefficients <-0.4 in all but one case (Table 10) ; reflecting the increase in scatter of residuals as clumping index decreases (Figure 8). The increased scatter may be due to a number of factors: SL2P produces greater random errors for spatially clumped canopies, land cover specific biases in SL2P, increased RM uncertainty for highly clumped canopies. Indeed, the covariation of land cover and clumping (Figure 5) makes it difficult to attribute cause to the observed increase in precision and uncertainty error as the clumping index decreases.

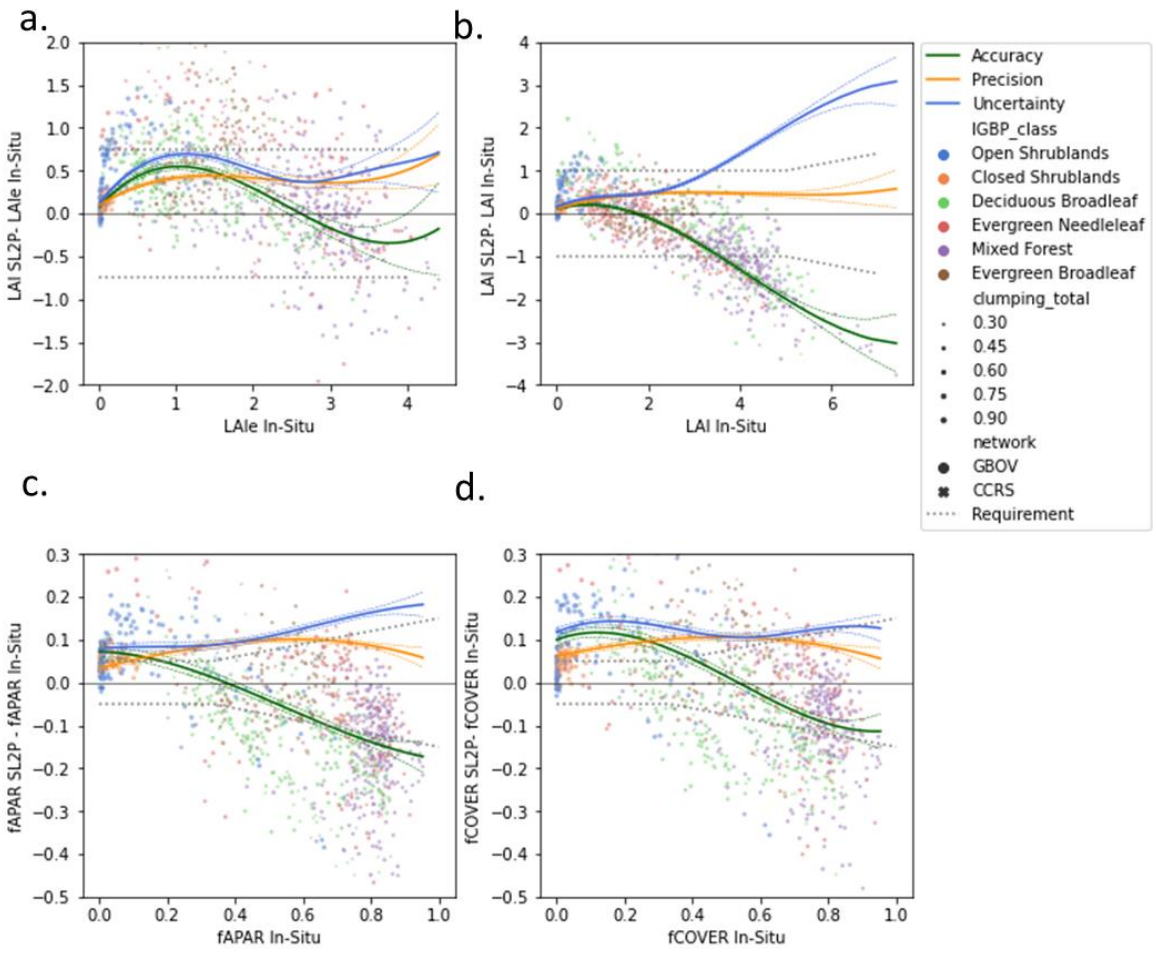

Figure 8. Residual plots of SL2P estimates versus matching RM as a function of RM value together with fitted models of Accuracy, Precision and Uncertainty (solid colours) and their 96%ile confidence intervals (dashed colours) Symbol shape indicates network, symbol colour indicates IGBP class and symbol size indicates clumping index. Dashed lines bound target user requirement around solid 1:1 line.

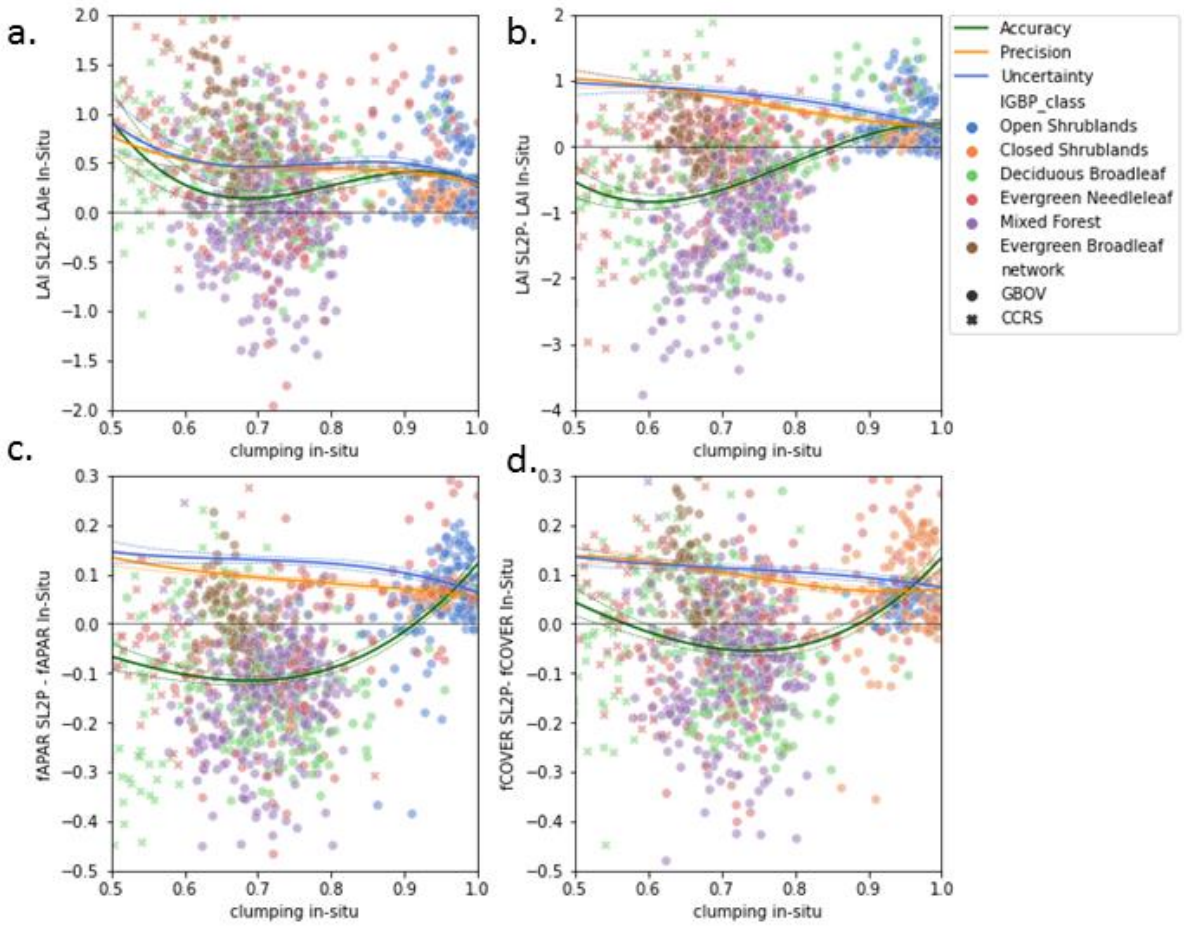

Figure 9. Residual plots of SL2P estimates versus matching RM as a function of clumping together with fitted models of Accuracy, Precision and Uncertainty (solid colours) and their 96%ile confidence intervals (dashed colours) Symbol shape indicates network, symbol colour indicates IGBP class.

Table 10. Pearson correlation coefficient between modelled A, P and U and in-situ clumping index for validated variables. All values significant at p<=0.002.

Variable	A	P	U
fAPAR	0.35	-0.54	-0.09
fCOVER	0.52	-0.63	-0.43
LAI	0.35	-0.68	-0.41
LAIe	-0.14	-0.65	-0.56

4.3.3 Validation of SL2P Theoretical Precision

For all variables, SL2P theoretical precision was poorly related to the P estimated from observed residuals (Figure 10). For LAIe and LAI, SL2P generally overestimates P with an almost uniform distribution below the 1:1 line. In contrast, SL2P theoretical precision was almost constant at ~.04 for fAPAR and fCOVER over forests and uncorrelated (r^2<0.1) with the modelled precision. It was only for fCOVER over shrublands that SL2P theoretical precision was relatively unbiased and within +/-0.05 of P.

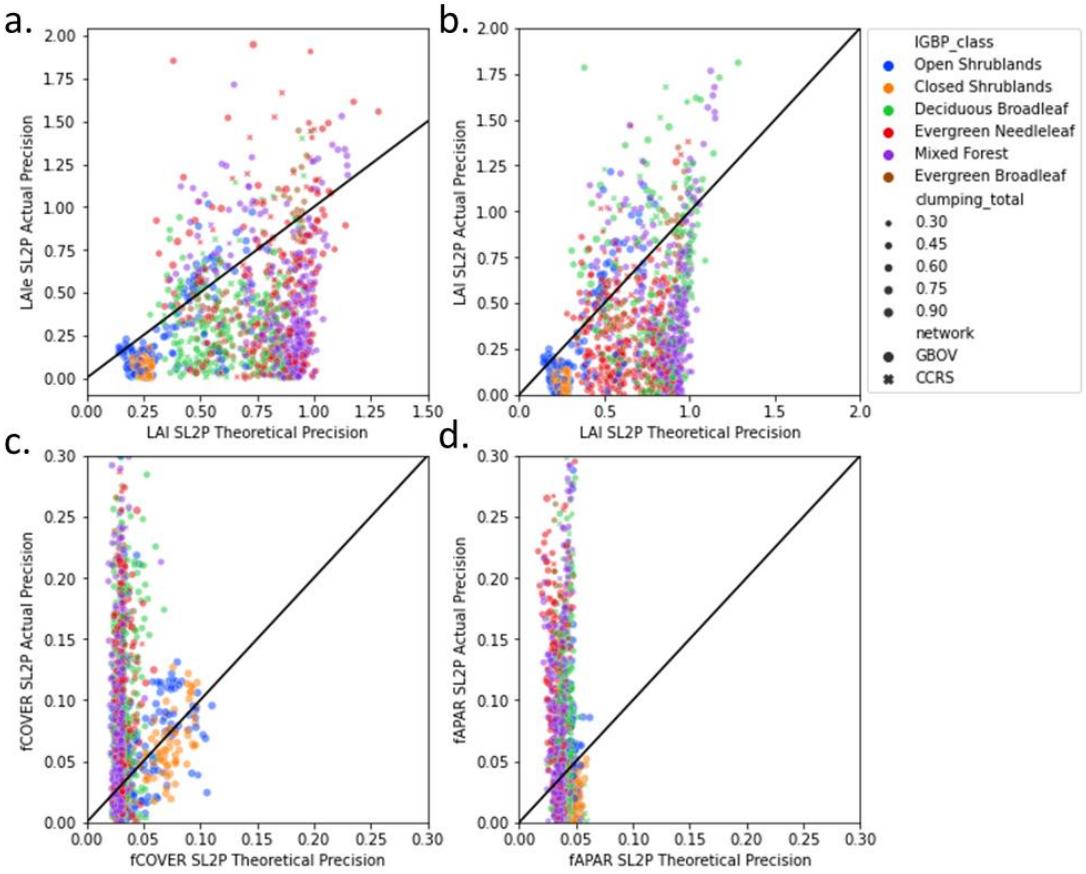

Figure 10. Scatter plots of SL2P modelled precision based on comparisons to RM versus theoretical precision based on the retrieval algorithm for in-situ sites. 1:1 line indicated in black.

4.4 Intercomparison

The number of intercomparisons for a given SL2P retrieval level ranged from 500 and 10000 for CGLS versus SL2P and from 1000 and 15000 (Figure 11). The larger number of MODIS comparisons was due to the higher temporal revisit frequency of MODIS on Aqua and Terra in comparison to the OLCI images on Sentinel 3a and 3b.

For brevity, we summarise intercomparison results across all ecozones since between ecozone variations were correlated to the magnitude of aggregated SL2P estimates (not shown) as expected from the relatively narrow conditional distributions of comparisons over all ecozones (Figure 12). MODIS and CGLS comparisons to SL2P were remarkably similar: both overestimate SL2P LAI by ~50% for 0.5<SL2P LAI<3.5 and fAPAR by ~20% for 0.2<fAPAR<0.8. However, MODIS and CGLS LAI and fAPAR saturated above these ranges while SL2P match-ups continued to increase. For low (<0.5) LAI and (<0.25) fAPAR, both MODIS and CGLS showed good agreement (within +/-0.25 LAI) with SL2P match-ups but were still overestimating SL2P fAPAR by between 0.05 and 0.1 units. Results for CGLS and SL2P fAPAR comparisons were similar to those for fCOVER as expected given the similarity of SL2P fCOVER and fAPAR (Figure 6) and the fact that CGLS fCOVER is a deterministic function of CGLS fAPAR.

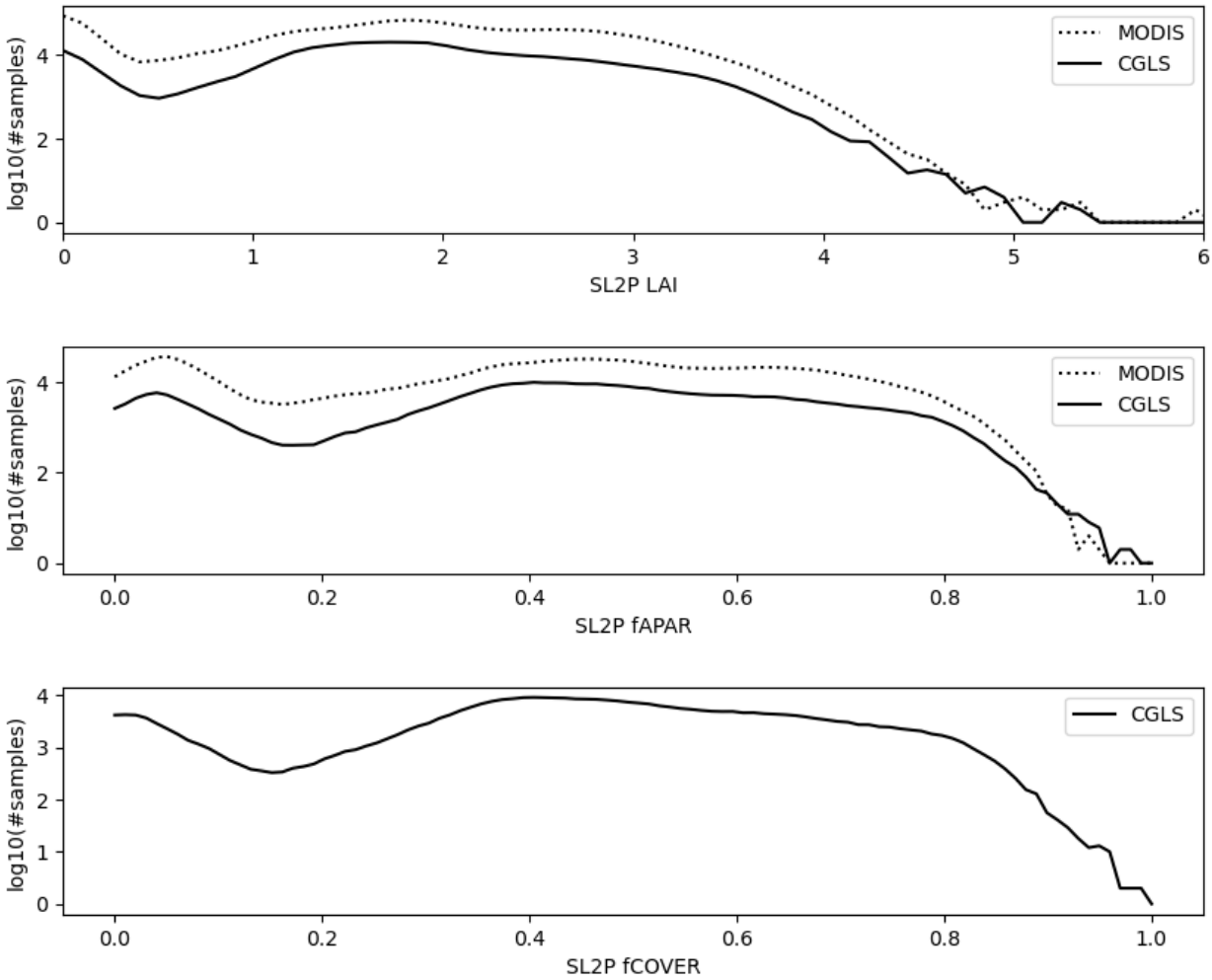

Figure 11. Number of comparisons (shown on a log10 scale) between aggregated SL2P retrieval and either MODIS or CGLS products over clear sky forest dominated 1.5km x 1.5km grid cells over intercomparison regions.

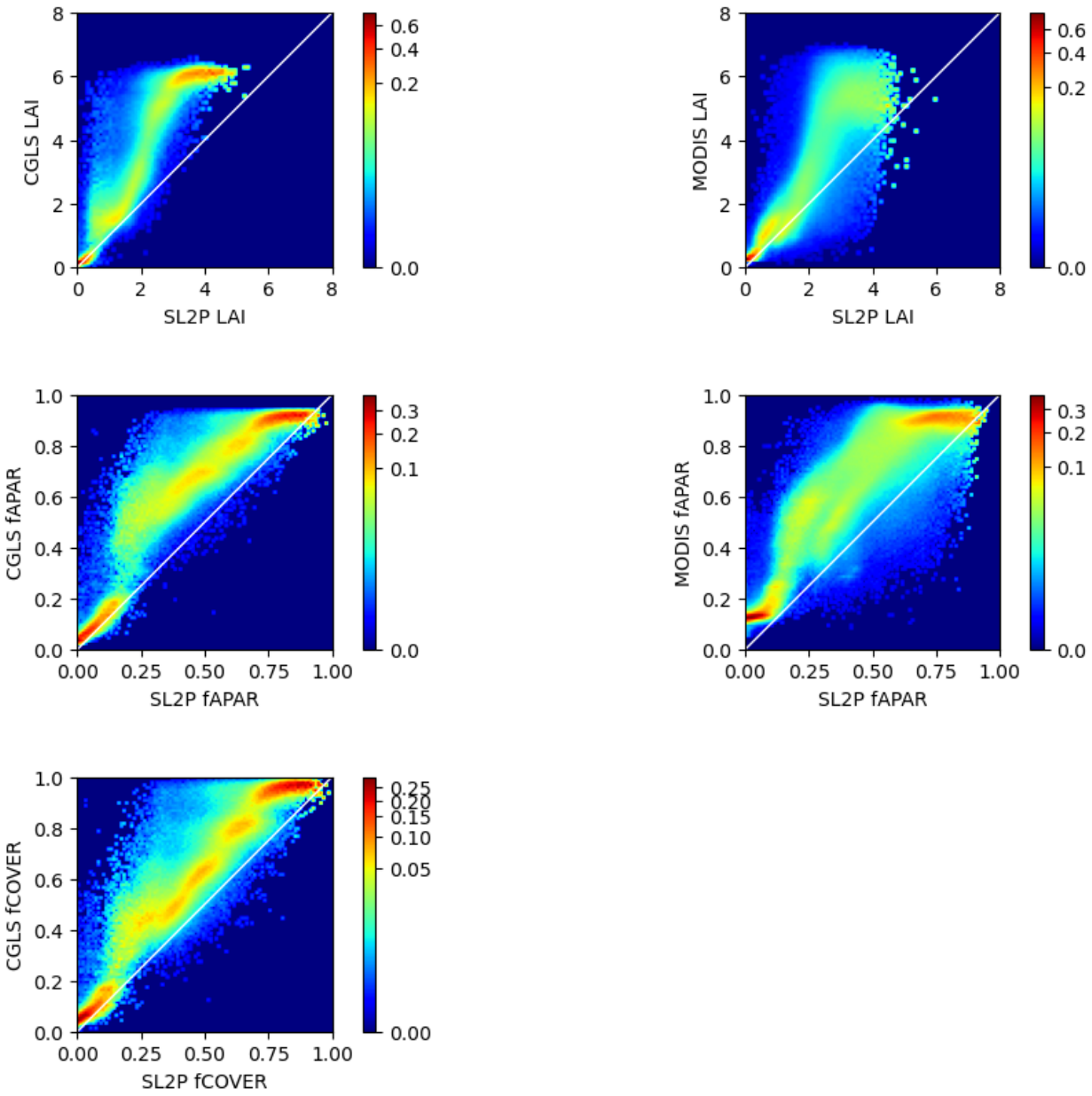

Figure 12. Density plots of the conditional probability of CGLS (left column) or MODIS (right column) comparisons given a matching aggregated SL2P estimate for 1.5km x 1.5km grid cells. Colours correspond to conditional probability of reference product variable given aggregated SL2P match-up value.

5.Discussion

It has been 20 years since the first continental scale validation of medium resolution satellite LAI products was conducted (Fernandes et al. 2003). Since then, algorithms for mapping canopy variables from medium resolution imagery have progressed but it is only recently that they have been implemented in a manner suitable for systematic large area mapping. Validation of outputs from these systems is critical both to assess fit for purpose and to prioritise improvements in algorithms or inputs.

This study focussed on SL2P both because it is being used for science and applications and it serves as a free and open baseline for benchmarking new approaches. We further considered forests because previous studies have shown SL2P typically meets user requirements over croplands but not over forests (Table 4). Brown et al. (2021) showed that SL2P underestimated forest LAI even with uniform calibration priors; pointing to a systematic limitation in either L2a inputs or PROSAILH. We hypothesized the lack of clumping within the PROSAILH was the cause of the bias as empirical algorithms using similar input imagery are unbiased for LAI over North American forests (Fernandes et al., 2003). We also needed to determine if the bias seen for LAI also occurred in fAPAR and fCOVER. To address these questions we expanded the limited spatial sample used in Brown et al. (2021) to include 133 new northern latitude forest ESUs at no small expense and also developed a validation approach appropriate to medium resolution products.

The RM dataset provided sampling over all but tropical forest ecozones. The latter are of global importance and should be incorporated in future validation but are of limited extent over North America. Comparison of our sampled range of each variable with previous studies (Surlock et al., 2001; Fernandes et al., 2003) indicate the data covered the typical range of LAI (0 to 7.5) across most North American forests with the exception of Douglas Fir forests on the Pacific coast that could approach values up to 10. On the other hand, this is the only study that validates SL2P over forests using a representative range of fAPAR and fCOVER. Simultaneous validation of all three variables is important since they are closely related in-situ (Figure 5) and for SL2P (Figure 6). Indeed, the close SL2P relationships suggest that there may be a benefit to using variables that are estimated with low bias (e.g. fCOVER) to constrain other variables such as LAI.

The CCRS network sites provided increased sampling of lower clumping index and a broader range of ecozones that used in Brown et al. (2021). This, together with intercomparison, allowed us to achieve a Level 3 validation recommended by CEOS for large area products. The CCRS sites provided broad spatial coverage but single date sampling while NEON sites the obverse. Current in-situ survey cannot provide both simultaneously and it seems that most networks prefer the latter since they are typically related to long term measurement sites. However, we suggest that a broad spatial sample is preferred, as it will eventually include temporal variability while a fixed network will never improve spatial coverage. Ideally, new technologies to permit automated regional estimates of RM using airborne surveys should be developed; especially those that include measurement approaches such as LIDAR or structure from motion that can map vertical canopy structure.

LAI validation indicated similar precision and bias as reported in Brown et al. (2021) but here included forests up to LAI 7.5. In contrast to LAI, we noticed a curious almost sinusoidal pattern to bias for other LAIe, fAPAR and fCOVER that shifted from positive to negative bias as they increased. This result may explain why previous studies found SL2P to be negatively biased for high fAPAR forests (Putzenlechner, et al., 2019) but relatively unbiased for moderate fAPAR over crops (Djamai et al., 2019). Our analysis also indicates that population level statistics can be misleading for bias and uncertainty and should be avoided in future good practice. All variables were estimated with relatively consistent precision that, in the absence of bias, would result in uncertainty falling within user requirements for most levels of each variable. This is encouraging since it indicates that the propagation of measurement error from inputs to product is modest. In fact, precision errors may even decrease further with temporal smoothing although this was beyond the scope of our study. The main challenge, especially for LAI, remains reducing bias.

Our attempt to test the hypothesis that SL2P LAI bias was due to clumping had mixed results. Qualitatively, SL2P resulted in larger LAI underestimates for the CCRS network versus the GBOV network for similar RM LAI (Figure 8). Given that the CCRS network also typically had lower clumping index (Figure 5) one may infer that LAI bias increases as spatial clumping increases. However, correlation analysis showed weak or even negative linear relationships between bias and increased spatial clumping (Table 8). The covariation of clumping with land cover and LAI (e.g. shrub clumping close to 1 in Figure 5) meant that we could not separate these two effects from clumping. Indeed, it may be impossible to control for these effects when using undisturbed sites and may require real or numerical canopy

manipulation experiments (e.g. Stenberg et al., 2014; Widlowski et al., 2015). An alternative would be to simply test if replacing PROSAILH in SL2P with an accurate heterogeneous radiative transfer model reduces bias since the model parameterization implicitly accounts with the covariation of other canopy variables. We still suggest that spatial clumping is the cause of LAI bias since LAIe bias is proportionally smaller in magnitude. At the same time, there is no evidence that clumping affects SL2P bias for fAPAR and fCOVER.

The theoretical precision of SL2P is not sufficiently accurate for fAPAR and fCOVER or precise for LAIe and LAI to be of any use (Figure 10). Indeed, it is contradictory to assume that precision could be predicted for each retrieval with low uncertainty since if that were the case one could use this prediction to improve retrievals. Nevertheless, one could expect an unbiased estimate of precision if cross validation was sufficiently robust during SL2P calibration. The current cross validation approach is to test retrievals for PROSAILH simulations drawn from the same priors used for calibration. At a minimum, precision should be modelled using different priors and ideally using an ensemble of model simulations. One alternative may be to use perturbations of paired RM and satellite measurements, based on the associated uncertainties, to quantify precision using the validation approach presented here.

SL2P underestimation of MCD15 and CGLS LAI agreed with the fact that SL2P underestimated in-situ LAI while these reference products are generally unbiased. However, we are hesitant to draw further insights for comparisons with CGLS for two reasons: i) CGLS retrievals of LAI and fAPAR are either heavily weighted to the MCD15 values for LAI>2 and essentially based on the SL2P algorithm for LAI<1 and ii) CGLS fCOVER is a functional transformation of CGLS fAPAR so fCOVER intercomparisons provide no new insights compared to fAPAR intercomparisons. This leaves SL2P versus MCD15 fAPAR as the remaining truly independent comparison. Here, SL2P shows a consistent underestimation of MCD15 fAPAR which itself is known to be relatively unbiased for fAPAR>0.5 and overestimates fAPAR<0.5 (Brown et al. 2020). These results are consistent with the bias we observed for SL2P with respect to in-situ data and suggest that while SL2P can be improved by reducing underestimation for fAPAR>0.5 it is MCD15 that may need improvement for lower fAPAR.

The intercomparison was limited to sample regions due to our initial concern regarding computation demands of having to generate SL2P products over larger areas. Ongoing work with GEE are generating Canada wide monthly SL2P products that could be extended globally with modest costs. This suggests

that future intercomparison could be done using exhaustive sampling. Additional sampling may be useful to understand product differences at high LAI where precision is low and for specific land cover conditions such as regeneration or disturbance. Areas with poor agreement could also be useful to focus new in-situ measurements. An objective approach is required to design a sampling design for these cases.

This study built on the large number of previous coarse resolution product validation studies (Table 5 and Table 6) as well as recent medium resolution validation studies (Table 4) to identify good practices for survey, code verification, validation, and intercomparison. However, there remain three elephants in the room when it comes to the practice of land parameter validation:

i. Agencies invest significant funding into observing systems, algorithm development, and services but limited amounts to the acquisition of reference measurements. Even GBOV, the Copernicus validation service, does not itself operate systematic survey systems other than for benchmarking survey methods. Satellite validation has relied primarily on long term networks. These may be sufficient for publishing a new algorithm but do not have enough spatial coverage to meet CEOS requirements. CEOS and reviewers of new systems and services need to require proof that quality can be assured within the design of new satellite observing systems.

Ii. There is no accepted approach to track the quality assurance of algorithms and mapping systems. ISO and IEEE standards are widely used for analogous systems across other industries but we have only seen such standards for radiative transfer models in terms of land surface mapping with satellite EO (Widlowski et al. 2015). The lack of standards can influence downstream services. For example, we the SNAP implementation of SL2P has yet to be updated to address the bugs identified in our study. CEOS is in a position to require developers to adopt standard and publish the level of standard met by various systems. This is especially important as future systems may not be in the public domain.

Iii. Both product generation and validation relies on computer code that is often not public. This prevents replication of results in an efficient and accurate manner and understanding if product differences are due to bugs in code. The MCD15 product had six revisions that vastly improved efficiency and performance. These revisions were enabled by public sector funding for validation and code updates. However, the MCD15 algorithm and its associated RT models are not published in a free and open manner so future science may have limited access to the progress of this work. We feel it is

critical for the scientific community and funding agencies to embrace the free and open publication of code (our code is available within the LEAF-Toolbox, Fernandes et al. 2020)

6. Conclusions

This study validated SL2P for mapping LAI, fAPAR and fCOVER over North American forests using Sentinel 2 Multispectral Instrument data. It enhanced previous studies by increasing the spatial coverage of in-situ reference measurements so they represented most forest ecozones, by quantifying thematic performance over all three variables simultaneously and by conducting product intercomparison. These steps and the publication of this work meet necessary conditions for CEOS Level 3 validation. The study had three goals: report on thematic performance of SL2P, determine if biases are due to clumping and provide new good practices.

Code verification of SL2P identified bugs in the SNAP implementation that affect both product retrieval and quality control flags. The SNAP implementation should not be used until revision. The verified SL2P implementation used here underestimated in-situ LAI by between 20% and 50% and MODIS LAI by ~50% for LAI>2. Compared to in-situ measurements, SL2P fAPAR and fCOVER bias trended from approximately +0.1 to -0.1 as both variables increased. The fAPAR underestimation was also observed when comparing to MODIS for fAPAR>0.5. Precision was relatively constant at <0.1 units for fAPAR and fCOVER and <0.5 units LAI. SL2P satisfied target uncertainty requirements for 48% of LAI, 37% of fCOVER and 31% of fAPAR comparisons to in-situ data. The low level of agreement reflects both biases in products and stringent requirements for fCOVER and fAPAR. Reducing product bias is fundamental to reducing thematic uncertainty.

Clumping showed only weak linear relationships ($|r^2|<0.5$) to bias for all variables and even these were at times counterintuitive, with bias increasing as canopies were less clumped. Our sample was not able to control for the covariation of clumping and the mapped variables to quantify the impact of clumping on SL2P bias. Further studies are required in disturbed landscapes or with simulations. Nevertheless, as in Brown et al. (2021) the fact that SL2P estimates LAIe with little or no bias but underestimates LAI still

suggests the absence of clumping in PROSAILH is to blame for LAI bias. Scatterplots of residuals also indicated the CCRS network sites tended to show greater negative LAI bias than the less clumped GBOV network sites at comparable LAI.

This study promoted new good practices for validation of canopy biophysical variables that may benefit future studies. Firstly, we acquired sufficient reference data to have a representative sample. Moreover, the data were based on networks that followed consistent acquisition and processing standard and that included uncertainty propagation. There are diminishing returns for exploiting data using non-standard instruments or methods even if they are theoretically superior to current networks unless uncertainty can be included. We further strongly feel that relying on long term networks alone can bias the sampling distribution of reference data and should always be augmented with spatially representative sampling. Second, we demonstrated the use of regression to model thematic performance as a function of the mapped value. For small sample sizes, this approach has greater objectivity and robustness in comparison to histogram methods and also provides uncertainties. Finally, we provide all code, including SL2P and the validation methods and data, in a free and open manner. This is fundamental to both replicate our work and to enhance future validation.

We conclude by noting that with the publishing of new algorithms and products is becoming both easier and more frequent with on-line journals and free and open computing platforms. These algorithms and products represent complex hypotheses about the physics and structure of our environment. The value of these hypotheses should be measured in our ability to test and potentially defeat them. Validation data, methods and the human activity of publishing the validation results is fundamental for users to understand the limitations of algorithms and products and for developers to make improvements.

7.Acknowledgements

We acknowledge Dr. W. Chen, Dr. Liming He, Dr. Robert Fraser, Dr. Julie Lovitt, Dr. H. Peter White, Dr. Yu Zhang, and xx for data collection. The work was funded by Natural Resources Canada's Earth Observation for Cumulative Effects Project and Canada Centre for Mapping and Earth Observation.

8.References

Baret,F., Hagolle, O., Geiger,B., Bicheron, P., Miras,B., Huc, M. , Berthelot,B. , Niño,F. , WeissM., Samain, O., Roujean,J.L. , Leroy, M. , 2007. LAI, fAPAR and fCover CYCLOPES global products derived from VEGETATION: part 1: principles of the algorithm. Remote Sens. Environ., 110, pp. 275-286

Baret , F., Weiss, M., Verger, A., and Smets, B., ATBD FOR LAI, FAPAR AND FCOVER FROM PROBA-V PRODUCTS AT 300M RESOLUTION (GEOV3), ImagineS, FP7-Space-2012-1, I1.73, https://land.copernicus.eu/global/sites/cgls.vito.be/files/products/ImagineS_RP2.1_ATBD-LAI300m_I1.73.pdf

Brown, L., Otougu, B. and Dash, J., 2019. Estimating Forest Leaf Area Index and Canopy Chlorophyll Content with Sentinel-2: An Evaluation of Two Hybrid Retrieval Algorithms, Remote Sens. 2019, 11(15), 1752; https://doi.org/10.3390/rs11151752.

Brown, L.A., Meier, C., Morris, H., Pastor-Guzman, J., Bai, G., Lerebourg, C., Gobron, N., Lanconelli, C., Clerici, M., Dash, J., 2020. Evaluation of global leaf area index and fraction of absorbed photosynthetically active radiation products over North America using Copernicus Ground Based Observations for Validation data, Remote Sensing of Environment, Volume 247, 111935, ISSN 0034-4257, https://doi.org/10.1016/j.rse.2020.111935.

Brown, L., Fernandes, R., Djamai, N., Meier, C., Gobron, N., Morris, H., Canisius, C., Bai, G., Lerebourg, C., Lanconelli, C., Clerici, M., Dash, J., 2021. Validation of baseline and modified Sentinel-2 Level 2

Prototype Processor leaf area index retrievals over the United States, IISPRS Journal of Photogrammetry and Remote Sensing, 175, 71-87, https://doi.org/10.1016/j.isprsjprs.2021.02.020.

Brown, L., Camacho, F., García-Santos, V., Origo, N., Fuster, B., Morris, H., Pastor-Guzman, J., Sánchez-Zapero, J., Morrone, R., Ryder, J., Nightingale, J., Boccia, V., & Dash, J., 202.. Fiducial Reference Measurements for Vegetation Bio-Geophysical Variables: An End-to-End Uncertainty Evaluation Framework. Remote Sensing, 13, 3194. https://www.mdpi.com/2072-4292/13/16/3194.

Commission for Environmental Cooperation, 2020. 2015 Land Cover of North America at 30 Meters", North American Land Change Monitoring System, Ed. 2.0. Accessed at http://www.cec.org/north-american-environmental-atlas/land-cover-30m-2015-landsat-and-rapideye/.

Commission for Environmental Cooperation, 2022. CEC Terrestrial Ecological Regions of North America, Montreal, Commission for Environmental Cooperation, accessed at http://www.cec.org/north-american-environmental-atlas/north-american-forests-2022/.

Defence Mapping Agency, 1990. DEFENSE MAPPING AGENCY TECHNICAL MANUAL 8358.1 DATUMS, ELLIPSOIDS, GRIDS, AND GRID REFERENCE SYSTEMS. DM ™ 8358.1, Defence Mapping Agency, U.S.A., http://everyspec.com/DoD/DOD-General/download.php?spec=DMA_TM-8358.1.006300.PDF.

Djamai, N., Fernandes, R., Weiss, M., McNairn, H., Goïta, K., 2019. Validation of the Sentinel Simplified Level 2 Product Prototype Processor (SL2P) for mapping cropland biophysical variables using Sentinel-2/MSI and Landsat-8/OLI data. Remote Sens. Environ., 225, 416-430, 10.1016/j.rse.2019.03.020.

Doxani, G., Vermote, E., Roger, J.-C., Gascon, F., Adriaensen, S., Frantz, D., Hagolle, O., Hollstein, A., Kirches, G, ; Li, F., Louis, J., Mangin, A., Pahlevan, N., Pflug, B., Vanhellemont, Q,. 2018. Atmospheric Correction Inter-Comparison Exercise. Remote Sens., 10, 352.

ESA Sentinel-2 Team, 2007. GMES Sentinel-2 Mission Requirments Document. EOP-SM/1163/MR-dr. European Space Agency. accessed at https://earth.esa.int/pub/ESA_DOC/GMES_Sentinel2_MRD_issue_2.0_update.pdf on January 20, 2021.

Fernandes, R. et al., 2021, "LEAF Toolbox", Canada Centre for Remote Sensing, https://github.com/rfernand387/LEAF-Toolbox/wiki, DOI: 10.5281/zenodo.4321298.

Fernandes, R., Canisius, F. et al. 2022. "In-Situ Leaf Area Index, fAPAR and Canopy Cover Measurements over Canadian Forests in Support of Cumulative Effects Assessments. Geomatics Canada Open File, in preparation.

Fernandes,F., Butson, C., Leblanc, S. and Latifovic, R., 2003.Landsat-5 TM and Landsat-7 ETM+ based accuracy assessment of leaf area index products for Canada derived from SPOT-4 VEGETATION data, Canadian Journal of Remote Sensing, 29:2, 241-258, DOI: 10.5589/m02-092.

Fuster B, Sánchez-Zapero J, Camacho F, García-Santos V, Verger A, Lacaze R, Weiss M, Baret F, Smets B, 2020. Quality Assessment of PROBA-V LAI, fAPAR and fCOVER Collection 300 m Products of Copernicus Global Land Service. Remote Sensing. 12, 1017. https://doi.org/10.3390/rs12061017.

Gascon F, Bouzinac C, Thépaut O, Jung M, Francesconi B, Louis J, Lonjou V, Lafrance B, Massera S, Gaudel-Vacaresse A, Languille F, Alhammoud B, Viallefont F, Pflug B, Bieniarz J, Clerc S, Pessiot L, Trémas T, Cadau E, De Bonis R, Isola C, Martimort P, Fernandez V., 2017. Copernicus Sentinel-2A Calibration and Products Validation Status. Remote Sensing. 2, 9, :584. https://doi.org/10.3390/rs9060584.

GCOS, 2019. Essential Climate Variables [WWW Document]. URL https://public.wmo.int/en/programmes/global-climate-observing-system/essential-climate-variables (accessed 5.2.19).

He, Li. , Chen, Ji., Pisek, J., Schaaf, C.B, and Strahler, A. (2012). Global clumping index map derived from the MODIS BRDF product. Remote Sensing of Environment. 119. 118-130. 10.1109/IGARSS.2011.6049427.

Hu, Q., Yang, Y., Xu, B., Huang, J.,. Memon, M.S., Yin, G., Zeng, Y.,. Zhao, J.,. Liu, K., 2020. Evaluation of global decametric-resolution LAI, FAPAR and FVC estimates derived from Sentinel-2 imagery. Remote Sens., 12, 912, 10.3390/rs12060912.

Janzen, D. et al., 2020. EO Baseline Data for Cumulative Effects Year End Report (FY 2019/20), Geomatics Canada Open File 60, available at https://publications.gc.ca/collections/collection_2020/rncan-nrcan/m103-3/M103-3-60-2020-eng.pdf.

Jin, H., Li, A., Bian, B., Nan, X., Zhao, W., Zhang, Z., Yin, G., 2017.Intercomparison and validation of MODIS and GLASS leaf area index (LAI) products over mountain areas: A case study in southwestern China,m International Journal of Applied Earth Observation and Geoinformation, 55, 52-67, https://doi.org/10.1016/j.jag.2016.10.008.

Kao, R.H., Gibson, C.M., Gallery, R.E., Meier, C.L., Barnett, D.T., Docherty, K.M., Blevins, K.K., Travers, P.D., Azuaje, E., Springer, Y.P., Thibault, K.M., McKenzie, V.J., Keller, M., Alves, L.F., Hinckley, E.-L.S. , Parnell, J., Schimel, D., 2012. NEON terrestrial field observations: designing continental-scale, standardized sampling. Ecosphere, 3, 10.1890/ES12-00196.1, art115.

Kganyago, M., Mhangara, P., Alexandridis,T, Laneve, G, Ovakoglou, G. 2020. Validation of sentinel-2 leaf area index (LAI) product derived from SNAP toolbox and its comparison with global LAI products in an African semi-arid agricultural landscape, Remote Sensing Letters 11 (10), 883-892.

Lambin, E.F. and Geist, H.J., 2006. Land-Use and Land-Cover Change. Local processes and Global Impacts. Lambin, E.F. and H.J. Geist (Eds). The IGBP Series, Springer-Verlag, Berlin, 222 pp/

Latifovic, R., Homer, C., Ressl, R., Pouliot, D.A., Hossian, S., Colditz, R., Olthof, I., Chandra, G., Victoria, A., 2012. North American Land Change Monitoring System. Remote Sensing of Land Use and Land Cover: Principles and Applications. 303-324. 10.1201/b11964-24.

Leblanc, S.G., Chen, J.M., Fernandes, R., Deering, D.W., Conley, A., 2005. Methodology comparison for canopy structure parameters extraction from digital hemispherical photography in boreal forests. Agricultural and Forest Meteorology 129 (3–4), 187–207

Lin, G., Wolfe, R., Zhang, P, Tilton, J., Dellomo, J., Tan, B., 2019. Thirty-six combined years of MODIS geolocation trending. Proc. SPIE 11127, Earth Observing Systems XXIV, 1112715 (9 September 2019); doi: 10.1117/12.2529447.

Monteith, J.L. and Unswirth, M.H., 2014. Principles of Environmental Physics, 4th ed. Academic Press, https://doi.org/10.1016/C2010-0-66393-0.

Nestola E, Sánchez-Zapero J, Latorre C, Mazzenga F, Matteucci G, Calfapietra C, Camacho F, 3017. . Validation of PROBA-V GEOV1 and MODIS C5 & C6 fAPAR Products in a Deciduous Beech Forest Site in Italy. Remote Sensing. ,9 :126. https://doi.org/10.3390/rs9020126

Müller-Wilm, U., 2018. Sen2Cor Configuration and User Manual (2nd ed.), CS, Toulouse, France.

Myneni, R., Knyazikhin, Y., Park, T., 2015. MCD15A3H MODIS/Terra+Aqua Leaf Area Index/FPAR 4-day L4 Global 500m SIN Grid V006 [Data set]. NASA EOSDIS Land Processes DAAC. Accessed 2021-04-19 from https://doi.org/10.5067/MODIS/MCD15A3H.006.

Putzenlechner, B., Castro, S.;, Kiese, R., Ludwig, R.;, Marzahn, P., Sharp, I., Sanchez-Azofeifa, A., 2019. Validation of Sentinel-2 fAPAR products using ground observations across three forest ecosystems. Remote Sens. Environ,, 232, 111310.

Radoux J, Chomé G, Jacques DC, Waldner F, Bellemans N, Matton N, Lamarche C, D'Andrimont R, Defourny P., 2016. Sentinel-2's Potential for Sub-Pixel Landscape Feature Detection. Remote Sensing., 8, :488. https://doi.org/10.3390/rs8060488.

Ryu, Y., Nilson, T., Kobayashi, H., Sonnentag,)., Law, B.E., Baldocchi,D.D., 2010.

On the correct estimation of effective leaf area index: Does it reveal information on clumping effects?,

Agricultural and Forest Meteorology,150, 463-472, https://doi.org/10.1016/j.agrformet.2010.01.009.

Sanchez-Sapero, J. and Martinez-Sanchez, E., 2022. QUALITY ASSESSMENT REPORT LAI, FAPAR, FCOVER FROM SENTINEL-3/OLCI COLLECTION 300M VERSION 1.1, Copernicus Global Land Operations – Lot 1, Issue: I1.20,https://land.copernicus.eu/global/sites/cgls.vito.be/files/products/CGLOPS1_QAR_LAI300m-V1.1_I1.20.pdf.

Scurlock, J., Asner, G.,Gower, S., 2001. Worldwide Historical Estimates of Leaf Area Index, 1932-2000. ORNL/TM-2001/268, Oak Ridge National Laboratory, U.S.A.
bhttps://info.ornl.gov/sites/publications/Files/Pub57077.pdf.

Stenberg P, Mõttus M, Rautiainen M, Sievänen R. 2014. Quantitative characterization of clumping in Scots pine crowns. Ann Bot., 114(4), 689-694, doi: 10.1093/aob/mct310.

Verger, A. and Descals, A., 2022. ALGORITHM THEORETICAL BASIS DOCUMENT Leaf Area Index (LAI) Fraction of Absorbed Photosynthetically Active Radiation (FAPAR) Fraction of green Vegetation Cover (FCover) Collection 300m Version 1.1, CGLOPS1_ATBD_LAI300m-V1.1 © CGLOPS Lot1 consortium,

https://land.copernicus.eu/global/sites/cgls.vito.be/files/products/CGLOPS1_ATBD_LAI300m-V1.1_I1.10.pdf

Verhoef,W., Jia, L., Xiao, Q. Su, Z., 2007. Unified optical-thermal four-stream radiative transfer theory for homogeneous vegetation canopies, IEEE Trans. Geosci. Remote Sens., 45 1808-1822,

Warren-Wilson, J., 1963. Estimation of foliage denseness and foliage angle by inclined point quadrats, Aust. J. Bot., 11, 95-105.

Weiss, M., Baret,F. Block, T.,Koetz, B., Burini, A., Scholze, B., Lecharpentier, P., Brockmann, C., Fernandes, R., Plummer, S., Myneni, R., Gobron, N., Nightingale, J., Schaepman-Strub, G., Camacho de Coca, F., Sanchez-Azofeifa, G.A>., 2014. On Line Validation Exercise (OLIVE): A Web Based Service for the Validation of Medium Resolution Land Products. Application to FAPAR Products. Remote Sensing. 6. 4190-4216. 10.3390/rs6054190.

Weiss, M., Baret, F., 2016. S2ToolBox Level 2 Products: LAI, FAPAR, FCOVER, 1.1. ed. Institut National de la Recherche Agronomique, Avignon, France. https://step.esa.int/docs/extra/ATBD_S2ToolBox_L2B_V1.1.pdf.

Widlowski, J.L. Mio, C. Disney, M. Adams, J. Andredakis, I. Atzberger, C. Brennan, J. Busetto, I. Chelle, M. Ceccherini, G. et al., 2015. The fourth phase of the radiative transfer model intercomparison (RAMI) exercise: actual canopy scenarios and conformity testing. Remote Sens. Environ., 169, pp. 418-437.

Wolfe, R., Roy, D. and Vermote, E. 1998. MODIS land data storage, gridding and compositing methodology: Level 2 Grid. IEEE Trans Geosci Remote Sens, 36, 1324-1338.

Yamazaki D., Ikeshima, D., Tawatari, R., Yamaguchi, T., O'Loughlin, F., Neal, J.C., Sampson, C.C., Kanae, S. and Bate, P.D., 2017. . A high accuracy map of global terrain elevations. Geophysical Rese arch Letters, vol.44, pp.5844-5853, 2017. doi:10.1002/2017GL072874

Yan K, Park T, Yan G, Liu Z, Yang B, Chen C, Nemani RR, Knyazikhin Y, Myneni RB, 2016. Evaluation of MODIS LAI/FPAR Product Collection 6. Part 2: Validation and Intercomparison. Remote Sensing., 8, 460. https://doi.org/10.3390/rs8060460

Yang et al., 2006. MODIS Leaf Area Index Products: From Validation to Algorithm Improvement.IEEE Trans.Geosci.RemoteSens.,44, 1885–1898.